7118–7136 *Nucleic Acids Research, 2017, Vol. 45, No. 12* *Published online 25 April 2017*
doi: 10.1093/nar/gkx281

Methyl-CpG binding domain protein 1 regulates localization and activity of Tet1 in a CXXC3 domain-dependent manner

Peng Zhang[1], Cathia Rausch[1], Florian D. Hastert[1], Boyana Boneva[1], Alina Filatova[2], Sujit J. Patil[1], Ulrike A. Nuber[2], Yu Gao[3], Xinyu Zhao[3] and M. Cristina Cardoso[1,*]

[1]Cell Biology and Epigenetics, Department of Biology, Technische Universität Darmstadt, Schnittspahnstrasse 10, 64287 Darmstadt, Germany, [2]Stem Cell and Developmental Biology, Department of Biology, Technische Universität Darmstadt, Schnittspahnstrasse 10, 64287 Darmstadt, Germany and [3]Waisman Center & Department of Neuroscience, University of Wisconsin-Madison, Madison, WI 53705, USA

Received August 10, 2016; Revised March 30, 2017; Editorial Decision April 04, 2017; Accepted April 06, 2017

ABSTRACT

Cytosine modifications diversify and structure the genome thereby controlling proper development and differentiation. Here, we focus on the interplay of the 5-methylcytosine reader Mbd1 and modifier Tet1 by analyzing their dynamic subcellular localization and the formation of the Tet oxidation product 5-hydroxymethylcytosine in mammalian cells. Our results demonstrate that Mbd1 enhances Tet1-mediated 5-methylcytosine oxidation. We show that this is due to enhancing the localization of Tet1, but not of Tet2 and Tet3 at heterochromatic DNA. We find that the recruitment of Tet1 and concomitantly its catalytic activity eventually leads to the displacement of Mbd1 from methylated DNA. Finally, we demonstrate that increased Tet1 heterochromatin localization and 5-methylcytosine oxidation are dependent on the CXXC3 domain of Mbd1, which recognizes unmethylated CpG dinucleotides. The Mbd1 CXXC3 domain deletion isoform, which retains only binding to methylated CpGs, on the other hand, blocks Tet1-mediated 5-methylcytosine to 5-hydroxymethylcytosine conversion, indicating opposite biological effects of Mbd1 isoforms. Our study provides new insights on how cytosine modifications, their modifiers and readers cross-regulate themselves.

INTRODUCTION

In mammals, the fifth position of cytosine can be modified by DNA methyltransferases to 5-methylcytosine (5mC) (1,2). The majority of 5mC is present in the context of CpG dinucleotides (CpGs) (3). Constitutive heterochromatin, which is usually marked by high levels of 5mC, is highly condensed and clustered in mouse cells forming the so-called chromocenters (4,5).

The 5mC can specifically be recognized by 5mC readers, and methyl-CpG binding domain (MBD) proteins represent one such family of proteins. Until now, five members of the MBD protein family have been well characterized including Mbd1, Mbd2, Mbd3, Mbd4 and Mecp2. Except for Mbd3, all members can specifically recognize methylated CpGs (5,6). The binding of MBD proteins to methylated CpGs regulates gene expression and chromatin structure (7).

While the MBD domain mediates binding to methylated CpGs, their unmethylated counterparts can be specifically recognized by the CXXC domain protein family (8). Although members of the CXXC domain protein family share a conserved CXXC motif, which contains two cysteine-rich clusters, three types of CXXC domain proteins are further classified according to sequence similarities. Only type one can specifically recognize unmethylated CpGs, type two and type three show less or no specificity for unmethylated CpGs (9). Interestingly, Mbd1, which contains a MBD, also belongs to the CXXC domain protein family. Several isoforms of Mbd1 have been identified and the full length Mbd1 contains three CXXC domains. However, only the third CXXC domain can specifically recognize unmethylated CpGs (10–12). An increasing number of studies show that the CXXC domain proteins may act as a CpG island targeting module (8,13,14).

Recent studies showed that 5hmC, the oxidation product of ten–eleven translocation proteins (Tet) (15), is not only involved in loss of DNA methylation (16) but also acts as a stable epigenetic mark (17) involved in the regulation of gene expression (18), cellular reprogramming (19) and embryonic stem cell (ESC) differentiation (20). The unique genomic pattern of 5hmC in different tissues, cells and de-

*To whom correspondence should be addressed. Tel: +49 6151 16 21882; Fax: +49 6151 16 21880; Email: cardoso@bio.tu-darmstadt.de

velopmental stages (21) indicates that Tet-mediated 5mC to 5hmC conversion is highly regulated. Indeed, several studies showed that the N-terminus of Tet1 itself (22,23), as well as post-translational modifications (24,25) and co-factors (26,27) regulate Tet1 activity. Genome wide analysis showed that Tet1 preferentially localizes to CpGs *in vivo* (18,22). However, the CXXC domain of Tet1 belongs to type three (9), which, as further shown by *in vitro* binding assays (28), has no specificity for CpGs. Accordingly, the localization of Tet1 to CpGs is more likely to be facilitated by other proteins. Previous studies showed that the CXXC domain of IDAX (29) specifically recognizes unmethylated CpGs and further recruits Tet2 to CpG sites, indicating that CXXC domain proteins might target Tet proteins to CpG sites.

Since Mbd1 has CXXC binding sites for both, methylated and unmethylated DNA (12), it is a potential candidate for targeting Tet1 to CpGs. In this study, we investigated the dynamics of Mbd1 and Tet1 by analyzing their subnuclear localization and the formation of the Tet oxidation product 5hmC. We show that Mbd1 enhances Tet1-mediated 5mC to 5hmC conversion by interacting with and facilitating its localization to methylated DNA. Subsequently, we find that catalytically active Tet1 displaces Mbd1 from methylated DNA. Finally, we show that recruitment of Tet1 by Mbd1 is not cell cycle dependent and requires the CXXC3 domain that binds unmethylated CpG. These results define the spatio-temporal network of interactions among the methylcytosine reader Mbd1, the methylcytosine modifier Tet1 and its oxidation products and the importance for regulation of chromatin organization.

MATERIALS AND METHODS

Expression plasmids

Plasmids coding for EGFP or EGFP tagged Mbd proteins were described in previous publications (30–33) and the corresponding fusion proteins are shown in Supplementary Figure S1. Mbd1 (pcDNA-Mbd1a), Flag-tagged Mbd1 with CXXC3 deletion (pFlag-Mbd1b) and pGBP-MaSat were described before (12,34). mCherry-tagged catalytic active (mCherry-Tet1CD: aa 1367–2007) and inactive (mCherry-Tet1CDmut: aa 1367–2007, H1652Y, D1654A) Tet1 were described before (35).

For construction of CFP-tagged human PCNA, the GFP coding sequence in the pENeGFPCNAL2mut (36) vector was replaced by the ECFP coding sequence from the pECFP-C1 vector (Clontech Laboratories, Inc., CA, USA) using AgeI and BsrGI restriction enzymes.

For construction of mCherry-tagged mouse Tet1, Np95 was replaced by Tet1 (28) in the mammalian expression vector pCAG-mCherry-Np95-IB (37) using AsiSI and NotI restriction sites.

For construction of mCherry-tagged mouse Tet2CD, Tet1CD was replaced by Tet2CD in the mCherry-Tet1CD vector using AsiSI and NotI restriction sites.

For construction of mCherry-tagged mouse Tet3CD, Tet1CD was replaced by Tet3CD in the mCherry-Tet1CD vector using AsiSI and NotI restriction sites.

For construction of GFP-tagged mouse Mbd1.2 (pmMbd1.2G, TRD (Mbd1), aa 396–636), the sequence coding the C-terminus of Mbd1 (Mbd1 and GFP) was amplified from pFBMbd1a-GFP (31) using primers containing EcoRI and XbaI sites. Then, the fragment was inserted into pEYFP-N1 (Clontech Laboratories, Inc., CA, USA) using EcoRI and XbaI restriction sites. The primers used were:

Mbd1.2 F: 5′- ATGAATTCATGCTGCAGTTTGCCATGAAGC-3′;

Mbd1.2 R: 5′-GATCTAGATTACTTGTACAGCTCG-3′.

For construction of GFP-tagged mouse Mbd1.3 (pG-mMbd1.3, Mbd1b, Mbd1ΔCXXC3), Mbd1b from p-FlagMbd1b was inserted into pEGFP-C3 (Clontech Laboratories, Inc., CA, USA) using HindIII and BamHI restriction sites.

For construction of GFP-tagged mouse Mbd1.4 (pG-mMbd1.4, Mbd1ΔMBD, aa 75–636), the sequence coding for Mbd1 lacking the MBD domain was amplified from pMbd1-GFP using primers containing HindIII and BamHI sites. Then, the fragment was inserted into pEGFP-C3 (Clontech Laboratories, Inc., CA, USA) using HindIII and BamHI restriction sites. The primers used were:

Mbd1.4 F: 5′- CATAAGCTTACTCATCCCTTGGC-3′;

Mbd1.4 R: 5′-AATGGATCCCAAAACTTCCTCCTT-3′.

For construction of GFP-tagged mouse Mbd1.5 (pG-mMbd1.5, MBD (Mbd1), aa 1- 98), the sequence coding for the MBD domain and NLS were amplified from pMbd1-GFP using primers containing HindIII and BamHI restriction sites. Then, the fragment was inserted into pEGFP-C3 (Clontech Laboratories, Inc., CA, USA) using HindIII and BamHI restriction sites. The primers used were:

Mbd1.5 F 5′- CATAAGCTTATGGCTGAGTCCTG-3′;

Mbd1.5 R: 5′- AATGGATCCCAGCCCAACCTG-3′.

For construction of GFP-tagged mouse Mbd1.7 (pG-mMbd1.7, Mbd1 (C289,292A)), the respective mutations were introduced with the Q5® Site-Directed Mutagenesis Kit (NEB, catalog #E0554S) according to the manufacturer´s instructions. The template for polymerase chain reaction (PCR) was the plasmid containing mouse Mbd1 (pMbd1-GFP) and the primers were:

F 5′-GCCGCTGCAGCCTGCCTACGGCGG-3;

R 5′-CCCAGCCTTGCGGTTCTGCCGCTGG-3.

Lenti-shMbd1 (pYG-21, pc3361) and lenti-shNC (negative control, (pYG-22, pc3362)) were cloned using lentivirus-sh-Control vector as backbone (38). Briefly, based on mouse Mbd1 mRNA sequence, shMbd1 (5′-GCTGCAGATCCAGACCTTTCA-3′) was designed using BLOCK-iT™ RNAi Designer software. The shNC sequence (5′-GGAATCTCATTCGATGCATAC-3′) was published previously (38). The shRNA sequences together with the loop sequence (TCAAGAG), U6 promoter and restriction sites (HpaI and ClaI) were cloned using two rounds of PCRs with Lenti-U6 promoter-miR-137 vector (38) as PCR template. The primers were:

shMbd1-3:

first round forward: 5′-GAATTCGGATCCGTTAACCAGGAAGAGGGCCTATTTCCCAT-3′

first round reverse: 5′-CCAGACCTTTCACTCTTGATGAAAGGTCTGGATCTGCAGCCGGATCCTCGTCCTTTCCAC-3′

second round forward: 5′-GAATTCGGATCCGTTAAC CAGGAAGAGGGCCTATTTCCCAT-3′
second round reverse: 5′-CTCCCAAGCTTATCGATA CAAAAAAGCTGCAGATCCAGACCTTTCACTCT TGATGAAAGG-3′
shNC:
first round forward: 5′-GAATTCGGATCCGTTAAC CAGGAAGAGGGCCTATTTCCCAT-3′
first round reverse: 5′-TTCGATGCATACCTCTTGAG TATGCATCGAATGAGATTCCCGGATCCTCGTC CTTTCCAC-3′
second round forward: 5′-GAATTCGGATCCGTTAAC CAGGAAGAGGGCCTATTTCCCAT-3′
second round reverse: 5′- CTCCCAAGCTTATCGATA CAAAAAAGGAATCTCATTCGATGCATACCTCTT GAGTATGCA-3′

The U6-shRNA cassettes were then cloned into lenti-U6-miR137 vector via HpaI and ClaI restriction sites using the In-fusion kit according to its instructions.

All plasmid constructs were verified by DNA sequencing and/or western blotting analyses.

Cell culture and transfection

HEK-293 (ATCC; catalog #CRL-1573) and HEK-EBNA (Invitrogen; catalog #620-07, Paisley PA4 9RF, UK) human cells were cultured and transfected using polyethylenimine as previously described (39).

For generation of an RFP-PCNA C2C12 stable cell line, plasmid pEN-CAG-mRFP-PCNA was transfected into C2C12 cells and the cells were selected with puromycin. mRFP positive and puromycin resistant cells were used for further experiments.

The mouse tail fibroblast (MTF) cell line was cultured using the conditions as previously described (40). Mouse wild-type (W8) embryonic fibroblasts (MEF) (41) and mouse *Dnmt1*$^{-/-}$ and *p53*$^{-/-}$ fibroblasts (42) were cultured as described before (43). These cells were transfected by nucleofection as previously described (44).

J1 mouse ES cells (2) and E14 mouse ES cells (45) were cultured under feeder-free conditions on gelatin coated culture dishes (0.2% gelatin in ddH_2O) in Dulbecco's modified Eagle's medium (high glucose) supplemented with 16% fetal bovine serum, 1× Minimum Essential Medium non-essential amino acids, 1× Penicillin/Streptomycin, 2 mM L-Glutamine (Sigma Aldrich, St Louis, MO, USA), 0.1 mM β-mercaptoethanol, 1000 U/ml LIF (Millipore), 1 μM PD0325901 and 3 μM CHIR99021 (Axon Medchem BV).

Confocal microscopy and image analysis

To calculate protein accumulation and colocalization, confocal Z stacks of live cells were acquired using the UltraView VoX spinning disc microscopy system (PerkinElmer Life Sciences) equipped with an oil immersion 60× Plan-Apochromat numerical aperture 1.45 objective lens as described before (34). Then, single mid-plane images were used for further analysis. To calculate protein accumulation, the mean intensity of five random regions inside and outside chromocenters was measured with ImageJ and the ratio of the mean gray value inside chromocenters to the mean gray value outside chromocenters was calculated. To measure the protein colocalization, *H*-coefficient analysis was performed as described before (46).

To follow the localization of Tet1 and Mbd1, MEF cells transfected with mCherry-Tet1CD and Mbd1-GFP constructs were used for time-lapse microscopy using the UltraView VoX spinning disc microscopy system. Cells were imaged every 90 min taking care to minimize laser exposure.

To evaluate the binding kinetics of fluorescently tagged proteins, fluorescence recovery after photobleaching (FRAP) was performed using the UltraView VoX spinning disc microscopy system. Quantitative evaluation was performed using ImageJ, and fluorescence intensity normalization and curve fitting were performed with the easyFRAP software as described before (44). T-half values were extracted from the mean exponential fitting, and plots were generated with RStudio (Version 0.99.893).

For the *in vivo* protein recruiting/interaction assay, *Dnmt1*$^{-/-}$ and *p53*$^{-/-}$ MEF cells were transfected with mCherry-Tet1CD, GFP-Mbd1 with or without the GBP-MaSat construct and 8 h after transfection, confocal Z stacks were acquired using the UltraView VoX spinning disc microscopy system. Then, protein accumulation tests were performed as described above.

High content screening microscopy spot analysis

To evaluate the distribution of proteins inside the cell nucleus, live cell experiments were performed using high content screening microscopy (Operetta, PerkinElmer, UK) with a 40× 0.45 numerical aperture long working distance objective (PerkinElmer, UK), a Xenon fiber optic as light source, 460–490 and 560–580 nm excitation filters and 500–550 (EGFP) and 590–640 (mCherry) emission filters, respectively. Eight hours after transfection, fluorescence signals were detected over a period of 20 or 24 h in time intervals of 4 h at 37°C with 5% CO_2. Harmony (Version 3.5.1, PerkinElmer, UK) software was used to perform image analysis. Briefly, the cell nuclei were identified by either Mbd or Tet signal and spots inside cell nuclei in each channel were identified. Then, the spot numbers, mean intensity of spots and mean intensity of cell nuclei were calculated per cell in the cell population with normal morphology, which is defined by cell roundness (round cell) and cell size (middle size). Last, calculated intensities were further processed and plotted using RStudio (Version 0.99.893) (Supplementary Figure S5).

To calculate cell numbers with Tet1 or Mbds accumulating at heterochromatic DNA, relative intensity (the ratio of spot and nucleoplasm intensity) above a given threshold was used for identifying the spots. Then, the percentage of cells with high spot numbers and low spot numbers were plotted.

To calculate the accumulation of Tet protein in heterochromatic DNA, the heterochromatic region was identified by Mbd1 relative intensity inside the cell nucleus (Supplementary Figure S5). Then, the ratio of the Tet1 mean intensity inside heterochromatic region and inside the cell nucleus was plotted at the different time points.

To evaluate the effect of Tet1 protein on the localization of Mbd1 protein, the Mbd1 signal at heterochromatic DNA

was identified by the intensity of spots (Supplementary Figure S5). The ratio of Mbd1 mean intensity inside heterochromatic regions and inside the cell nucleus was plotted against Tet1 expression and time points.

Tet1 protein stability assay

MEF cells were transfected with GFP-tagged Mbd1 or Mbd2 and mCherry-tagged Tet1CD constructs. Eight hours after transfection, the cells were cultured in the presence or absence of cycloheximide and imaged every 4 h by high content microscopy. The fluorescence intensity of GFP and mCherry inside the cell nucleus was calculated using the Harmony software and further plotted using Rstudio.

Mbd1 knockdown and isoform-specific rescue assay

Lentiviral particles were produced by transfection of HEK293 cells using the pCI-VSVG and psPAX2 packaging plasmids (Addgene numbers 1733 and 12260) and pYG-21 resp. pYG-22 shRNA containing plasmids. Mouse J1 ESCs were transduced using lentivirus-containing supernatants and 8 μg/ml polybrene. Twenty-four hours after transduction, the medium was replaced with virus-free ESC medium and cells were fixed at the indicated time points.

For Mbd1 isoform specific rescue, cells were transfected via nucleofection 48 h after transduction with Mbd1-GFP, GFP- Mbd1ΔCXX3 or GFP, respectively and fixed 24 h after transfection.

Immunofluorescence and image analysis

MEF or MTF cells were fixed for 10 min in 4% formaldehyde in phosphate buffered saline (PBS) and permeabilized for 20 min with 0.5% Triton X-100.

For detection of genomic 5hmC, cells were further fixed with ice-cold methanol for 5 min. After RNaseA (Qiagen, Germany) treatment (10 μg/ml in PBS) for 30 min at 37°C, cells were washed and blocked for 60 min in 0.2% fish skin gelatin (Sigma Aldrich, St Louis, MO, USA) in PBS at 37°C. Then 5hmC was detected using a rabbit anti-5hmC (1:250; catalog #39769, Active Motif, La Hulpe, Belgium) antibody together with 25 U/ml DNaseI (Sigma Aldrich, St Louis, MO, USA) in 1 × DNase buffer (10 mM Tris-HCl, 2.5 mM $MgCl_2$, 0.5 mM $CaCl_2$) and 2% bovine serum albumin (BSA) for 70 min at 37°C. To stop DNaseI digestion, cells were washed three times with PBS containing 1 mM ethylenediaminetetraacetic acid (EDTA) and 0.05% Tween. Following incubation with AMCA conjugated donkey anti-rabbit IgG (1:100; catalog #711-155-152, The Jackson Laboratory, Bar Harbor, ME, USA) secondary antibody for 50 min at room temperature. After three times washing with PBS containing 0.05% Tween (PBST) the cells were mounted in Vectashield medium (Vector Labs, Burlingame, CA, USA).

To detect Flag tagged Mbd1, a mouse anti-FLAG M2 (1:400; catalog #F3165, Sigma Aldrich, St. Louis, MO, USA) primary antibody and an Alexa Fluor 488 conjugated goat anti-mouse IgG (1:250; catalog #715-545-151, The Jackson Laboratory, Bar Harbor, ME, USA) were used.

To detect endogenous Mbd1, a mouse anti-Mbd1 B5 (1:75; catalog #sc-25261, Santa Cruz Biotechnology, Dallas, TX, USA) primary antibody and an Alexa Fluor 594 conjugated donkey anti-mouse IgG (1:300; catalog #715-585-151, The Jackson Laboratory, Bar Harbor, ME, USA) were used.

To detect endogenous Tet1 protein, MEF or MTF cells were transfected with the mCherry-Tet1CD construct. Twenty-four hours after transfection, immunostaining with a Tet1-specific antibody (24) was performed as described above. Mouse ESCs (E14) were immunostained with the same Tet1 antibody. Fixation, permeabilization, RNaseA treatment and blocking were performed as described for the 5hmC staining. Subsequently, the cells were incubated with a rat anti-Tet1 (5D8, 1:1) (24) in 2% BSA for 70 min. After three times washing with PBST, the cells were incubated with an Alexa Fluor 488 conjugated donkey anti-rat lgG (1:500, catalog #712-545-153, The Jackson Laboratory, Bar Harbor, ME USA) for 50 min at room temperature. Then, DNA was counterstained with 4′,6-Diamidine-2-phenylindole dihydrochloride (DAPI, 1 μg/ml).

mCherry, GFP or Alexa Fluor 488 and AMCA signals were imaged using high content screening microscopy with 20× 0.45 numerical aperture long working distance objective (PerkinElmer, UK), a Xenon fiber optic as light source, 360–400, 460–490 and 560–580 nm excitation filters and 410–480 (AMCA, DAPI), 500–550 (GFP, Alexa Fluor 488) and 590–640 (mCherry) emission filters, respectively. The images were further analyzed with Harmony software and plotted with RStudio. To test the effect of Mbds on 5hmC formation, we first grouped the cells by GFP/Mbds protein levels into low and high expressing fractions. Then, in each group, cells were further binned by Tet1 protein levels. The average 5hmC intensity of single cells was plotted. To measure the effect of Mbd1 on 5hmC formation in the cells with low Tet1 protein level, cells were first grouped by Tet1 protein level and, then, in each group, cells were further binned by GFP or Mbd1 protein level into low, middle and high expressing groups. Then, single cell 5hmC intensity was plotted.

To compare Tet1 protein levels, the fluorescence intensity of ectopic Tet1 (mCherry) and anti-Tet1 antibody was measured with high content screening microscopy using the same exposure time as before (Figures 1 and 5; Supplementary Figure S2). For MTF and MEF cells, the cells were grouped as in Supplementary Figure S2 according to mCherry-Tet1CD intensity. Then, total fluorescence intensity of the whole cell nucleus of single cells was plotted according to mCherry-Tet1CD mean intensity. As a comparison, total fluorescence of whole cell nucleus of mESC was also plotted.

Radioactive β-glucosyltransferase (BGT) assay

MEF cells were co-transfected via nucleofection with mCherry-Tet1CD and Mbd1-GFP, GFP-Mbd1ΔCXXC3 or GFP. Twenty-four hours later, cells were harvested, gDNA was isolated and the radioactive β-glucosyltransferase assay was performed as previously described (35) with the exception that 5 μg of genomic DNA were used for the reaction.

Protein interaction assay and isoform analysis

All buffers for protein interaction assays were supplemented with the protease inhibitors: AEBSF 1 mM (AppliChem; Darmstadt, Germany), E64 1 mM (Sigma-Aldrich, St Louis, MO, USA) and Pepstatin A 1 nM (Sigma-Aldrich, St Louis, MO, USA).

HEK-EBNA cells plated in p100 cell culture dishes were co-transfected with mCherry-Tet1CD and GFP-tagged subdomains of Mbd1 constructs. Forty-eight hours after transfection, the cell pellets were incubated in 500 μl of PARP buffer (2.5 mM Tris pH 8.0, 0.5 M NaCl, 50 mM glucose, 10 mM EDTA, 0.2% Tween, 0.2% NP40) for 10 min on ice. Following 10 times syringe (ø0.8, five times, followed by five times, ø0.6) treatment and another 10 min incubation, cell lysates were centrifuged at 13 400 × *g* for 20 min at 4°C. After centrifugation, 25 μl of the supernatant was aliquoted for Mbds/GFP input (input 2) and the rest was diluted with 500 μl of PARP buffer without NaCl and was incubated with RFP binding protein coupled to sepharose beads (RFP-Trap, ChromoTek, Planegg-Martinsried, Germany) supplemented with 10 μg/ml of ethidium bromide (EtBr) for 1 h at 4°C on a rotary shaker. After incubation, the beads were washed six times with PARP buffer containing 0.25 M NaCl. Next, the proteins were denatured at 99°C in sodium dodecyl sulphate (SDS) containing buffer (1% SDS, 25 mM Tris pH 6.8, 5% glycerol, 0.005% Bromophenol blue, 50 mM Dithiothreitol) for 10 min. Sodium dodecyl sulphate-polyacrylamide gel electrophoresis (SDS-PAGE) was used to separate proteins. After blotting to nitrocellulose membrane, the gel was stained with Coomassie Brilliant Blue as an input estimation for Tet1 protein (input 1). The GFP signals were detected with a rat monoclonal anti GFP (clone 3H9) primary antibody (31) (ChromoTek, catalog #029762, Planegg-Martinsried, Germany) and horseradish peroxidase conjugated goat anti rat IgG secondary antibody (1:5000, catalog #112-035-068, The Jackson Laboratory, Bar Harbor, ME, USA). To visualize the signal, ECL plus western blot detection reagent (GE Healthcare, München, Germany) was used and signals were detected on a chemiluminescence imager (Amersham imager 600 RGB), equipped with a CCD camera fitted with a large aperture f/0.85 FUJINON™ lens (GE Healthcare, München, Germany).

To further test the interaction of mCherry-Tet1CD with Mbd1-GFP, mCherry-Tet1CD and Mbd1-GFP or GFP were purified from Sf9 cell as described before (31). Immobilized mCherry-Tet1CD was incubated with similar amounts of Mbd1-GFP or GFP in PARP buffer containing 0.5 M NaCl and 10 μg/ml of EtBr for 1 h at 4°C on a rotary shaker. After incubation, the beads were washed and proteins were separated by SDS-PAGE. After blotting to nitrocellulose membrane, the gel was stained with Coomassie Brilliant Blue as an input estimation for Tet1 protein. Then, GFP signals were detected as described above.

To analyze the endogenous amounts of Mbd1 isoforms, 1 × 10^7 J1 mESCs were lysed, separated via SDS-PAGE and blotted to a nitrocellulose membrane as described above. Mbd1 and actin were detected with rabbit anti-Mbd1 M254 (1:100, catalog #sc-10751, Santa Cruz Biotechnology, Dallas, TX, USA) and mouse anti-actin AC-40 (1:1000, catalog #A4700, Sigma Aldrich, St Louis, MO, USA) primary antibodies and horseradish peroxide conjugated goat anti-rabbit IgG (1:10000, catalog #A0545, Sigma Aldrich, St Louis, MO, USA) and sheep anti-mouse IgG (1:5000, catalog #NA931, Amersham Pharmacia Biotech, UK) secondary antibodies. To compare the endogenous and the ectopically expressed Mbd1 isoforms, lysates of HEK-293 cells transfected with Mbd1 and Flag-Mbd1ΔCXXC3 were analyzed together with ESC lysates by 8% SDS-PAGE and western blot with anti-Mbd1 antibody as described above.

Statistical analyses and graphical representation

Independent two-group student's *t*-tests were performed using RSudio (Version 0.99.893) and *P*-values were indicated on the plots for all experiments, except for FRAP experiments where Wilcoxon tests were used.

Boxplots represent the median with the box depicting the 25–75 percentiles and the lines and dots 95% confidence interval and outliers, respectively.

RESULTS

Mbd1 enhances Tet1-mediated 5hmC formation

We have shown before that Mbd2 and Mecp2 but not Mbd3 counteract the ability of Tet1 to modify 5mC (35). To investigate whether Mbd1 affects Tet1-mediated 5hmC formation, MTF cells were co-transfected with mCherry-tagged Tet1CD (catalytic domain of Tet1) and GFP-tagged Mbd (methyl-CpG binding domain) proteins (Mbd1, Mbd2, Mbd3, Mbd4 and Mecp2) (Supplementary Figure S1). Twenty-four hours after transfection, cells were fixed and stained with an antibody against 5hmC. As expected, 5hmC levels increased proportionally to Tet1CD protein levels in control transfected cells co-expressing GFP alone (Supplementary Figure S2). While 5hmC levels were not affected in the cells expressing low Mbd protein levels (Supplementary Figure S2, left), 5hmC signals were decreased in cells expressing high Mbd2 and Mecp2 protein levels (Supplementary Figure S2, right) (35). High expression levels of Mbd3 and Mbd4, in contrast, resulted in similar 5hmC levels as obtained for the control cell with GFP expression (Supplementary Figure S2). These results indicate that Mbd2 and Mecp2 block Tet1-mediated 5hmC formation in a dose-dependent manner, while Mbd3 and Mbd4 do not affect Tet1-catalyzed 5mC oxidation. In contrast to Mecp2, Mbd2, Mbd3 and Mbd4, co-expression of Mbd1 resulted in a significantly increased 5hmC formation (Supplementary Figure S2, right). The gain in 5hmC was most pronounced in cells expressing low Tet1CD protein levels (Supplementary Figure S2, right, arrow) and, thus, we further focused on these cells (Figure 1A). Importantly, the Tet1 protein levels of these cells are equivalent to endogenous Tet1 protein levels in mouse ESCs (Supplementary Figure S3). As shown in Figure 1B, 5hmC levels positively correlated with GFP-tagged Mbd1, but not with GFP levels. Moreover, cells expressing Mbd1 showed significantly higher 5hmC levels than cells expressing GFP. These results indicate that under physiological levels of Tet1 protein, Mbd1 enhances Tet1CD-mediated 5hmC formation. In contrast, 5hmC lev-

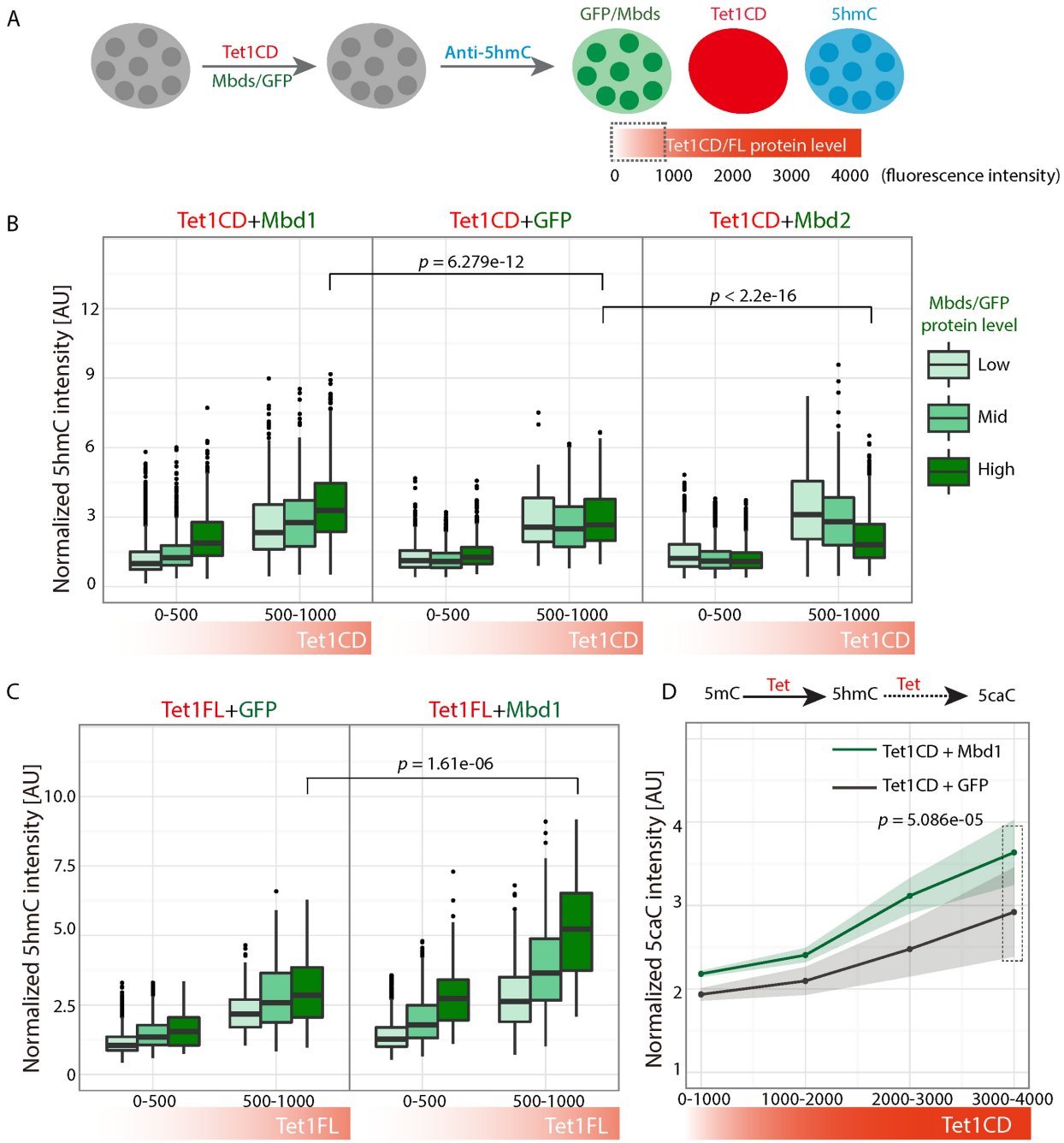

Figure 1. Mbd1 enhances Tet1-mediated 5hmC formation. (**A**) Experimental rationale. Mouse tail fibroblasts (MTF) were transfected with mCherry-Tet1CD (catalytic domain of Tet1) or mCherry-Tet1FL (full length Tet1) together with Mbd1-GFP (methyl-CpG binding domain protein 1), Mbd2-GFP or GFP. Twenty-four hours after transfection the cells were immunostained with a 5-hydroxymethylcytosine (5hmC) specific antibody. The signals of Tet1, Mbd/GFP and 5hmC were detected by high content screening microscopy and low Tet1 expressing cells were used for plotting. (**B**) Effect of Mbd1, Mbd2 and GFP on Tet1CD-mediated 5hmC formation. The cells were first grouped according to Tet1 protein levels, then, in each group, cells were further binned by Mbd/GFP protein levels and single cell intensities were plotted. The 5hmC intensities in the cells with high levels of Mbds/GFP and high levels of Tet1CD were used to perform student's *t*-test and *P*-values are indicated. Experiments were repeated at least three times. Cell numbers for Tet1CD + Mbd1, Tet1CD + GFP and Tet1CD + Mbd2 are 10817, 7271 and 4375, respectively. (**C**) Effect of Mbd1 and GFP on Tet1FL-mediated 5hmC formation in mouse embryonic fibroblast cells (MEF). Intensities of single cells are plotted and the *P*-value of student's *t*-test is indicated. Experiments were repeated at least two times. Cell numbers for Tet1FL + Mbd1 and Tet1FL + GFP are 7515 and 3429, respectively. (**D**) Effect of Mbd1 and GFP on Tet1-mediated 5-carboxylcytosine (5caC) formation in MTF cells. MTF cells were transfected with mCherry-Tet1CD together with Mbd1-GFP or GFP. Twenty-four hours after transfection, the cells were immunostained with an 5caC antibody. The average intensity of single cells was plotted according to Tet1CD protein levels. Experiments were repeated twice and mean values were plotted. Cell numbers for Tet1CD + Mbd1 and Tet1CD + GFP are 1770 and 582, respectively. The 5caC intensities in the cells with high levels of Tet1CD (dashed line box) were used to perform student's *t*-test and the *P*-value is indicated. 95% confidence intervals were also indicated in the plot.

els anti-correlated with the amount of Mbd2, which is in agreement with its 5mC protection ability.

The N-terminal domain of Tet1 is dispensable for its catalytic activity but it was shown to regulate Tet activity (22,23). As mentioned earlier, Tet1 contains a CXXC domain in its N-terminus (47), which cannot bind to DNA *in vitro* (28). To test whether Mbd1-mediated enhancement of 5hmC formation depends on the N-terminal domain of Tet1, mouse fibroblast cells were transfected with the mCherry-tagged full length Tet1 protein together with Mbd1-GFP or GFP, respectively. Twenty-four hours after transfection, cells were fixed and stained for 5hmC as previously described (Figure 1B). Similar to Tet1CD, 5hmC levels positively correlated with Mbd1 protein levels, but not with GFP and cells expressing Mbd1 showed significantly higher 5hmC levels than cells expressing GFP (Figure 1C), indicating that the N-terminal domain of Tet1 does not affect the Mbd1-mediated enhancement of 5hmC formation.

5hmC is not the only Tet1 oxidation product as it can be further converted to 5-formylcytosine (5fC) and 5-carboxylcytosine (5caC) in an iterative reaction. To test whether the Mbd1-dependent increase in 5hmC levels was not due to blocking its further conversion, MTF cells ectopically expressing mCherry-Tet1CD together with Mbd1-GFP or GFP were immunostained for 5caC. As shown in Figure 1D, 5caC levels were higher in the presence of Mbd1, indicating that Mbd1 does not block the further conversion of 5hmC to 5caC.

Taken together, these results indicate that Mbd1 enhances Tet1-mediated 5mC to 5hmC conversion and this is independent of the N-terminal domain of Tet1. Moreover, the increased 5hmC levels are not due to blocking of its further oxidation.

Mbd1 facilitates the efficient localization of Tet1 to methylated DNA

Oxidation of 5mC to 5hmC by Tet proteins involves several steps including DNA binding by a Watson–Crick polar hydrogen bond and van der Waals interactions, 5mC base flipping and 5mC to 5hmC oxidation (48,49). Therefore, the interaction between Tet1 proteins and DNA is a crucial initial step for Tet oxidation. Since Mbd1 enhances Tet1-mediated 5hmC formation, we wanted to test whether Mbd1 would affect interaction of Tet1 and DNA.

We first measured the dose and time dependency of the Tet1 oxidation reaction in *in vivo* experiments. At identical Tet1 protein levels, 5hmC amounts increased over time (Supplementary Figure S4). However, 5hmC levels were also proportional to Tet1 levels at both, early and late time points (Supplementary Figure S4). These results indicate that the Tet1-mediated formation of 5hmC depends on enzyme dose and oxidation time. We hypothesize that at early time points, in the presence of excess 5mC substrate, Tet1–DNA interactions predominate relative to later time points, where most of the substrate is oxidized. Thus, we performed live cell experiments 8 h after transfection to test the localization of Tet1 proteins.

In mouse cells, Mbd1 and Mbd2 proteins are mostly localized at highly methylated pericentric heterochromatin (HC). Confocal microscopy analysis showed that Tet1 proteins colocalize with Mbd1 at heterochromatic DNA, but not with Mbd2 (Figure 2A). To quantify the colocalization of Tet1 and Mbd proteins, *H*-coefficient (46) analysis was performed. As shown in Figure 2B, the colocalization between Tet1 and Mbd1 was significantly higher than that between Tet1 and Mbd2. In addition, we measured the accumulation of Tet1 proteins to heterochromatic DNA by quantifying the fluorescence signal of Tet1 proteins inside and outside heterochromatin. We found that co-transfection of Mbd1 but not Mbd2, significantly increased the accumulation of Tet1 proteins to heterochromatic DNA (Figure 2C). Altogether, these data show that Mbd1 enhances Tet1CD localization to heterochromatic regions. To further validate this, we performed high content microscopy screening spot analysis (Supplementary Figure S5A and B). Since Mbd1 protein is mostly accumulated at heterochromatin, one spot would represent one heterochromatic region in the cell. The results showed that the accumulation of Tet1CD at heterochromatic DNA, as well as 5hmC levels correlate with the amount of Mbd1 proteins (Supplementary Figure S6A and 7), indicating that Mbd1 enhances Tet1-mediated 5hmC formation by facilitating its localization to heterochromatic DNA in a dose-dependent manner. Similar to the catalytic domain of Tet1, Mbd1 enhances the heterochromatin accumulation of Tet1FL (Supplementary Figure S6B and 7), indicating that the N-terminal domain of Tet1 is dispensable for its Mbd1-mediated subnuclear localization.

Since Tet1-mediated 5mC oxidation depends on enzyme dose and Mbd1 enhances this process, we further tested whether Mbd1 could stabilize Tet1 proteins from degradation. To this end, we analyzed Tet1 stability in the presence of Mbd1 or, as a control, Mbd2. As shown in Supplementary Figure S8, Mbd1 did not enhance the stability of Tet1CD protein, therefore this cannot be the cause for increased 5hmC.

In mammalian cells, three Tets have been reported. Since we observed that Mbd1 enhanced Tet1CD localization at heterochromatic DNA, we further tested whether Mbd1 could also enhance Tet2 and Tet3 localization at heterochromatic DNA at an early time point (8 h after transfection). To this end, we measured the accumulation of Tet2CD and Tet3CD in the presence of Mbd1. As shown in Supplementary Figure S9, the accumulation of Tet1CD was significantly higher than the accumulation of Tet2CD and Tet3CD in the presence of Mbd1, indicating that the Mbd1 enhanced heterochromatin localization of Tet protein is specific for Tet1.

The accumulation of Tet1 proteins to heterochromatic DNA prompted us to investigate whether Tet1 DNA binding kinetics are affected. To this end, we performed fluorescence recovery after photobleaching (FRAP) analysis to measure the mobility of Tet1 proteins. We co-transfected MTF cells with mCherry-Tet1CD and Mbd2-GFP or Mbd1-GFP constructs. Eight hours after transfection, FRAP measurements were performed. Compared to freely nuclear distributed Tet1CD, heterochromatin accumulated Tet1 had much slower recovery kinetics (Figure 2D) and, thus, decreased mobility. Hence, we hypothesize that the prolonged retention time of Tet1 proteins at hete-

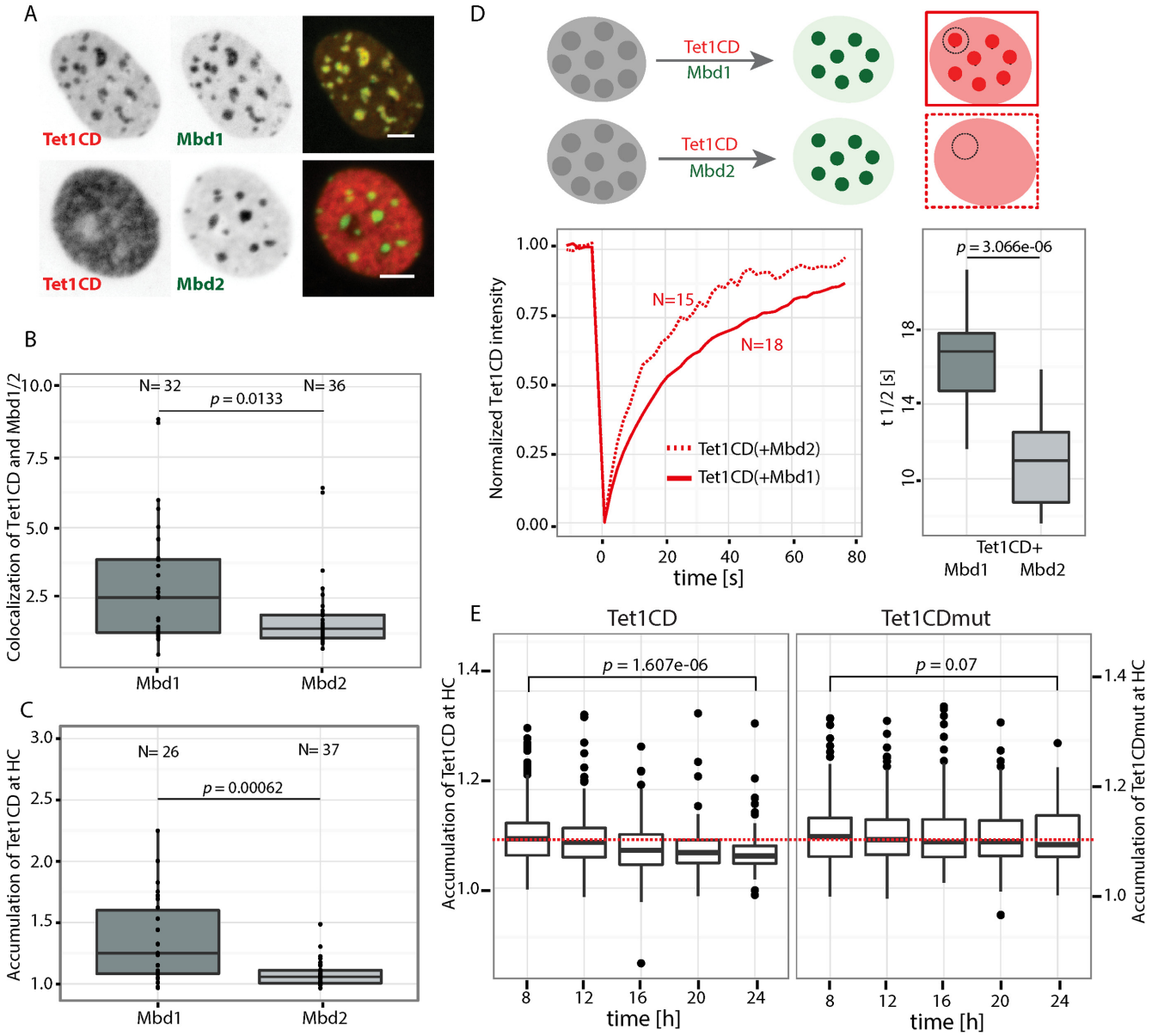

Figure 2. Mbd1 facilitates the localization of Tet1 to heterochromatic DNA. (**A**–**C**) Localization of Tet1CD and Mbd1 or Mbd2 in MTF cells. (A) MTF cells were transfected with Tet1CD together with GFP-tagged Mbd1 or Mbd2 constructs. Eight hours after transfection, Tet1 and Mbd1/Mbd2 signals were detected by confocal microscopy and images were used for *H*-coefficient colocalization (B) and protein accumulation (C) analysis. To calculate protein accumulation at heterochromatin, mean fluorescence intensities inside and outside heterochromatin were measured with ImageJ and the ratio of the mean gray value inside and outside heterochromatin was plotted. Scale bars: 5 μm. The cell number and *P*-values of the student's *t*-test are indicated. Two independent experiments were performed. (**D**) Fluorescence recovery after photobleaching (FRAP) analysis of Tet1 protein mobility. MEF cells were transfected with constructs coding for mCherry-Tet1CD together with Mbd1-GFP or GFP. The mCherry-Tet1CD signal at heterochromatin regions was photobleached with a 488 nm laser. The mean recovery curve was plotted. Cell numbers and *P*-value from Wilcoxon test are indicated on the plot. Two independent experiments were performed. (**E**) Accumulation of Tet1CD and Tet1CDmut (catalytic mutant of Tet1) to heterochromatic DNA. Shown are quantification results of the accumulation of Tet1 proteins at heterochromatic DNA using images from high content screening time-lapse microscopy. To better visualize the accumulation changes, the median accumulation value of Tet1CD at an early time point (8 h after transfection) is indicated and *P*-values of the student's *t*-test are indicated. Two independent experiments were performed. For each time point, more than 100 cells were analyzed.

rochromatic DNA allows an increased number of oxidation reactions.

The crystal structure of Tet2 in complex with DNA revealed that Tet2 proteins contain three iron binding sites, which are conserved in all three Tet proteins (48,49). Since the oxidation ability of Tet1 proteins is abrogated through mutations of two iron binding sites (50), we tested whether mutation of these two sites affects the accumulation of Tet1 to heterochromatic DNA. To this end, cells were transfected with a catalytic mutant of Tet1 (H1625Y and D1654A, Tet1CDmut) (50) and its accumulation to heterochromatic DNA was quantified as described earlier (Supplementary Figure S5A and C). At an early time point after transfection, the accumulation of Tet1CDmut at heterochromatic DNA is similar to the accumulation of Tet1CD (Figure 2E; Supplementary Figures S7 and 10). While for Tet1CDmut, the extent of heterochromatin accumulation (defined by the Mbd1 signal) remained stable over time (Figure 2E), the accumulation of the catalytically active Tet1 protein significantly decreased with progressive oxidation time (Figure 2E). Since Tet proteins have a substrate preference for 5mC (51), we suggest that once the oxidation reaction is completed, Tet1 proteins no longer bound to heterochromatic DNA resulting in decreased accumulation of Tet1CD at heterochromatic DNA. Since the two iron binding sites are indispensable for Tet1-mediated 5mC oxidation, we suggest that the accumulation of Tet1 to heterochromatic DNA and the subsequent 5mC oxidation are two distinct steps, whereby iron binding sites are not involved in the protein accumulation at heterochromatin. Taken together, these results indicate that Mbd1 enhances Tet1-mediated 5hmC formation by promoting its accumulation to heterochromatic DNA. This accumulation is *per se* independent of Tet1 catalytic activity.

Cell cycle-independent Tet1 accumulation at heterochromatic DNA

Mbd1 has been shown to recruit the histone lysine N-methyltransferase SETDB1 to the large subunit of the chromatin assembly factor 1 to form a S-phase-specific complex (52), suggesting a role for Mbd1 during DNA replication. To test whether the subnuclear localization of Mbd1 to heterochromatic DNA is cell cycle dependent, we transfected cells stably expressing the cell cycle S-phase marker RFP-PCNA (proliferating cell nuclear antigen) with Mbd1-GFP and performed the spot analysis as described earlier (Supplementary Figure S5A and B). The distribution of PCNA is cell cycle dependent. In G1 or G2-phase, PCNA distributes homogenously in the cell nucleus, while in S-phase it localizes to DNA replication foci. Especially in late S-phase, PCNA accumulates at heterochromatin (53,54). While about 75% of the cell population presented Mbd1 accumulated at heterochromatin, only about 25% of all cells showed PCNA accumulating at heterochromatin (Supplementary Figure S11). These results indicate that Mbd1 accumulation at heterochromatin is independent of the cells being in late S-phase.

Since we had shown that Mbd1 enhances the localization of Tet1 to heterochromatic DNA (Figure 2), we tested whether this enhancement is cell cycle dependent. To this

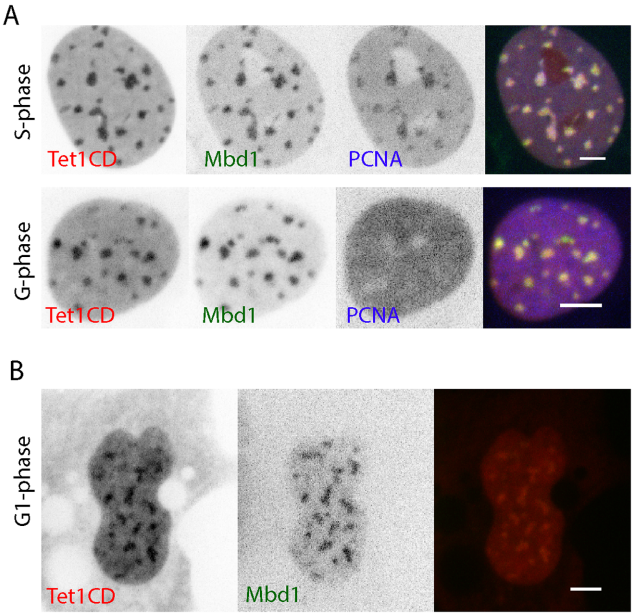

Figure 3. Mbd1 enhanced Tet1 localization to heterochromatic DNA is cell cycle independent. (**A**) Distribution of Tet1, Mbd1 and PCNA (proliferating cell nuclear antigen) in MEF cells. MEF cells were transfected with mCherry-Tet1CD, Mbd1-GFP and CFP-PCNA constructs. Eight hours after transfection, the live cells were imaged using confocal microscopy. The cell populations were discriminated by PCNA distribution to either (late) S-phase or G-phase. (**B**) Distribution of Tet1 and Mbd1 in G1-phase. Time-lapse microscopy was performed to follow cell division using the cells transfected with mCherry-Tet1CD and Mbd1-GFP (for full time lapse see Supplementary Video 1). Shown is an example of a cell in G1-phase. Scale bars: 5 μm.

end, MEF cells were transfected with CFP-PCNA, Mbd1-GFP and mCherry-Tet1CD, and the subnuclear localization of all three proteins was analyzed by confocal microscopy. In late S-phase, when PCNA accumulates at heterochromatin, colocalization with Tet1CD and Mbd1 was observed. In G1 or G2-phase, however, when PCNA distributes homogenously throughout the cell nucleus, Tet1 and Mbd1 were still bound to heterochromatic DNA (Figure 3A), indicating that Mbd1-enhanced accumulation of Tet1 to heterochromatin is not cell cycle dependent. To further analyze the distribution of Tet1 and Mbd1 throughout the cell cycle, time-lapse microscopy was performed with cells expressing mCherry-Tet1CD and Mbd1-GFP. Live cell imaging showed that before and after cell division, Tet1 and Mbd1 colocalize with each other (Figure 3B and Supplementary Video 1), indicating that the accumulation of Tet1 to heterochromatin in the presence of Mbd1 is not cell cycle dependent.

The interaction of Mbd1 and Tet1 enhances the localization of Tet1 to heterochromatic DNA

In MEF cells, about 80% of the major satellite DNA is methylated (43) and allows Mbd1 to bind and localize to heterochromatic regions mainly via its MBD domain (12). However, besides its MBD domain, the specific binding ability of the CXXC3 domain to unmethylated CpGs allows Mbd1 to localize to heterochromatic DNA in *Dnmt1*$^{-/-}$

cells (12), which were shown to have <20% methylation of the major satellite DNA (43). To test whether Mbd1-facilitated accumulation of Tet1 to heterochromatin is 5mC dependent, *Dnmt1*$^{-/-}$ MEF cells, ectopically expressing Tet1CD and Mbd1 were analyzed by confocal microscopy. As control, cells co-expressing Mbd2 and Tet1CD were used. The low level of residual DNA methylation in these cells lead to a very substantial decrease of the Mbd1 protein localization at major satellite DNA and an almost complete abrogation of the localization of Mbd2 (Figure 4A). As shown in Figure 4B (left, bar plot), Tet1 proteins did not accumulate to heterochromatic DNA in *Dnmt1*$^{-/-}$ cells expressing Mbd1 and Mbd2, respectively. Live cell microscopy experiments showed that the CXXC3 domain is necessary for localizing Mbd1 proteins to heterochromatic DNA in *Dnmt1*$^{-/-}$ cells (Supplementary Figure S12A). However, the efficiency of CXXC3-mediated localization of Mbd1 to heterochromatic DNA in *Dnmt1*$^{-/-}$ cells is much lower compared to that of the Mbd1 in wildtype cells (Supplementary Figure S12A and B). The levels of Mbd1 proteins accumulated at heterochromatic DNA in *Dnmt1*$^{-/-}$ cells might not be sufficient for Tet1 recruitment. These results indicate that Mbd1 enhances the localization of Tet1 to heterochromatin in a 5mC-dependent manner.

Previous studies have shown that a GFP-binding protein (GBP) fused to a polydactyl zinc finger major satellite DNA binding protein can target GFP-tagged proteins to major satellite heterochromatic DNA (Figure 4C) (34). To test whether artificially heterochromatin-tethered Mbd proteins can affect the subnuclear localization of Tet1, we subjected *Dnmt1*$^{-/-}$ cells that were triple transfected with mCherry-Tet1CD, GBP-MaSat and GFP-tagged Mbd1 or Mbd2 constructs to live cell microscopy. Compared to cells without GBP-MaSat transfection, GFP-tagged Mbd1 or Mbd2 were successfully targeted to heterochromatic DNA by GBP-MaSat, as assessed by an increased protein amount at heterochromatic DNA (Figure 4D). For cells co-expressing GFP-Mbd2 and mCherry-Tet1CD, we observed no colocalization of both proteins, while GFP-Mbd1 and mCherry-Tet1CD highly colocalized at heterochromatic DNA upon co-expression with GBP-MaSat (Figure 4D). Those results indicate that heterochromatin-tethered Mbd1 but not Mbd2 can recruit Tet1CD in *Dnmt1*$^{-/-}$ cells.

To further clarify whether the observed recruitment of Tet1CD by Mbd1 is mediated by direct protein–protein interactions, HEK cells expressing mCherry-Tet1CD and GFP-tagged deletion mutants of Mbd1 were subjected to co-immunoprecipitation (co-IP) experiments. To disrupt potential protein–DNA interactions, ethidium bromide was added to the interaction buffer (55). Although Tet1CD interacted with all deletion mutants of Mbd1, the strongest interaction was observed in the presence of the MBD domain (Figure 4E). Since Mbd1 and Tet1 are DNA binding proteins, purified proteins were used for *in vitro* co-IPs, to further exclude a DNA-bridged interaction. The interaction between Tet1 and Mbd1 could still be detected (Supplementary Figure S12C), indicating that Mbd1 physically interacts with Tet1 *in vitro*. To further validate these interactions, we ectopically tethered GFP tagged Mbd1 mutants to major satellite heterochromatic DNA as described above (Figure 4D) and analyzed colocalization of co-expressed mCherry-Tet1CD. The results showed that Tet1CD had a stronger interaction with the Mbd1 mutant containing the MBD domain (Supplementary Figure S12D), which is in agreement with the co-IP data.

Taken together, these results indicate that direct protein–protein interactions between Mbd1 and Tet1 favor the recruitment of Tet1 to heterochromatic DNA.

The CXXC3 domain of Mbd1 is necessary for the recruitment of Tet1 to heterochromatic DNA

In murine cells, different Mbd1 isoforms lacking the CXXC3 domain were found alongside with full length Mbd1 (10,11). The CXXC3 domain of Mbd1 is able to bind unmethylated CpG sites, which allows Mbd1 to specifically bind to unmethylated CpG-rich DNA. To test whether the ability to bind unmethylated CpG sites affects the localization of Tet1 proteins to heterochromatic DNA, MEF cells expressing mCherry-Tet1CD and GFP-tagged Mbd1 or Mbd1ΔCXXC3 (Figure 5A) were used for live cell microscopy experiments. Spot analysis showed more cells with Tet1 at heterochromatin in the presence of Mbd1 compared with Mbd1ΔCXXC3 (Supplementary Figure S13A, upper row). Moreover, as shown in Figure 5B and C, accumulation of Tet1 to heterochromatic DNA was increased in the presence of overexpressed Mbd1 compared to Mbd1ΔCXXC3 (Figure 5B and C; Supplementary Figure S13A, lower row). Similar results were obtained with full length Tet1 protein (Supplementary Figure S13B). In summary, these results indicate that the CXXC3 domain of Mbd1 is necessary for an enhanced localization of Tet1 to heterochromatic DNA.

Next, we tested the effect of the CXXC3 domain on Tet1-mediated 5hmC formation. To this end, MEF cells overexpressing Tet1CD and Mbd1 or Mbd1ΔCXX3 were used for *in situ* 5hmC stainings. In contrast to what we measured in Mbd1-transfected cells, 5hmC signal was lower in cells overexpressing Mbd1ΔCXXC3 (Figure 5D). Similar to Mbd2 (Figure 1B), 5hmC levels decreased with increasing Mbd1ΔCXXC3 levels (Figure 5D), indicating that Mbd1 proteins lacking the CXXC3 domain protect from Tet1-mediated 5mC to 5hmC conversion and CXXC3 is necessary to enhance Tet1-mediated 5hmC formation. To exclude any effects of Mbd1 on chromatin accessibility resulting in a changed 5hmC antibody access to DNA, we radioactively labeled and quantified 5hmC in genomic DNA of MEF cells, ectopically expressing mCherry-Tet1CD and GFP-tagged Mbd1 or Mbd1ΔCXXC3 (Supplementary Figure S14). The results of this radioactive assay perfectly agreed with the antibody based 5hmC detection.

Previous studies showed that point mutations of CXXC3 alone can abolish the binding of Mbd1 to unmethylated CpGs (56). Hence, we generated CXXC3 point mutants (Supplementary Figure S15A) and tested their effect on Tet1-mediated 5hmC formation as before (Figure 5). First, by spot analysis, we showed that the number of cells with Mbd signal localized at heterochromatin in *Dnmt1* knockout cells was higher in the presence of Mbd1 when comparing with Mbd1(C289,292A) (Supplementary Figure S15B and C). This indicated that the double mutations in CXXC3 domain indeed abolished the binding ability of Mbd1 to unmethylated heterochromatic DNA. Then, we measured the

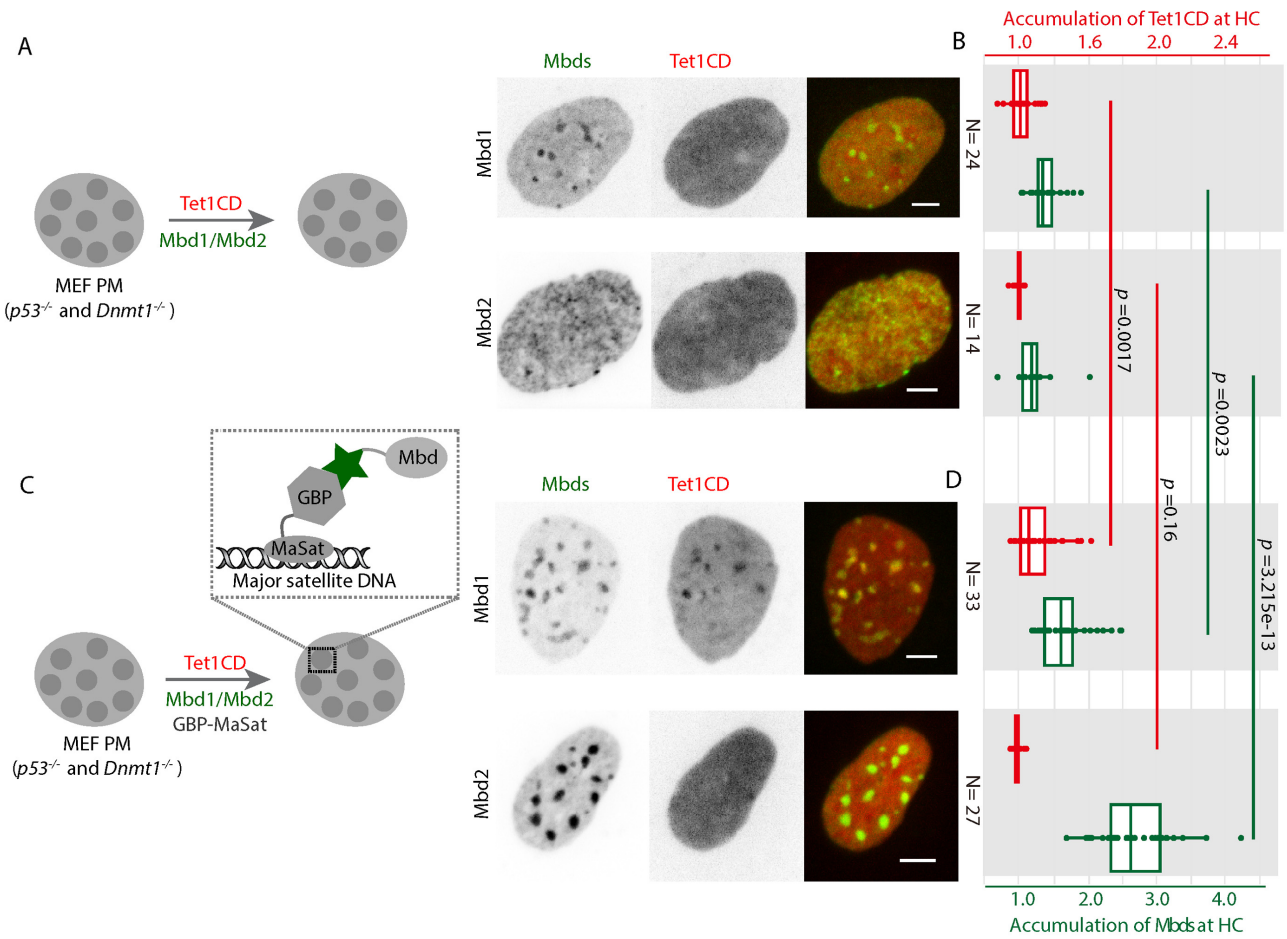

E

input 1 immobilized mcherry-Tet1CD	input 2 Anti GFP	interaction Anti-GFP		interaction efficiency
			Mbd1 GFP MBD TRD	++
			Mbd1ΔCXXC3 GFP MBD TRD	++
			Mbd1ΔMBD GFP TRD	+
			TRD (Mbd1) TRD GFP	+/-
			GFP GFP	-
			"beads" control	-

Figure 4. The interaction of Mbd1 and Tet1 enhances Tet1 localization to heterochromatic DNA. (**A**) *Dnmt1*$^{-/-}$ MEF (*p53*$^{-/-}$ and *Dnmt1*$^{-/-}$) cells were transfected with mCherry-Tet1CD and Mbd1-GFP or Mbd2-GFP. Eight hours after transfection, the cells were imaged using confocal microscopy. The left panel shows the schematic of the experiment and the right panel shows exemplary cells with Tet1 and Mbd1/Mbd2 expression. (**B**) Accumulation of Mbd1/Mbd2 and Tet1 proteins to heterochromatic DNA measured as in Figure 2. (**C**) *Dnmt1*$^{-/-}$ MEF cells were triple-transfected with mCherry-Tet1CD, GBP-MaSat (GFP binding protein, polydactyl zinc finger major satellite binder) and Mbd1-GFP or Mbd2-GFP plasmids. Eight hours after transfection, cells were imaged using confocal microscopy. The left panel shows the schematic of the experiment and how GBP-MaSat targets GFP-tagged proteins to heterochromatic DNA. The right panel shows exemplary cells with Tet1 and Mbd1/Mbd2 expression in the presence of GBP-MaSat. (**D**) Accumulation of Tet1 and Mbd1/2 proteins to heterochromatic DNA. Cell number and *P*-value of *t*-test are indicated. (**E**) Interaction between Tet1CD and subdomains of Mbd1. HEK (human embryonic kidney) cells co-expressing mCherry-Tet1CD and GFP tagged Mbds were used for co-immunoprecipitation assays using immobilized RFP binding protein. The input and bound GFP signals on the membrane were detected using a GFP-specific antibody. Left panels are input for mCherry and GFP fusion proteins and rightmost panel shows interaction bands. The middle panel depicts the structures of Mbd1 fusions. The right panel summarizes the results of two independent biological replicates.

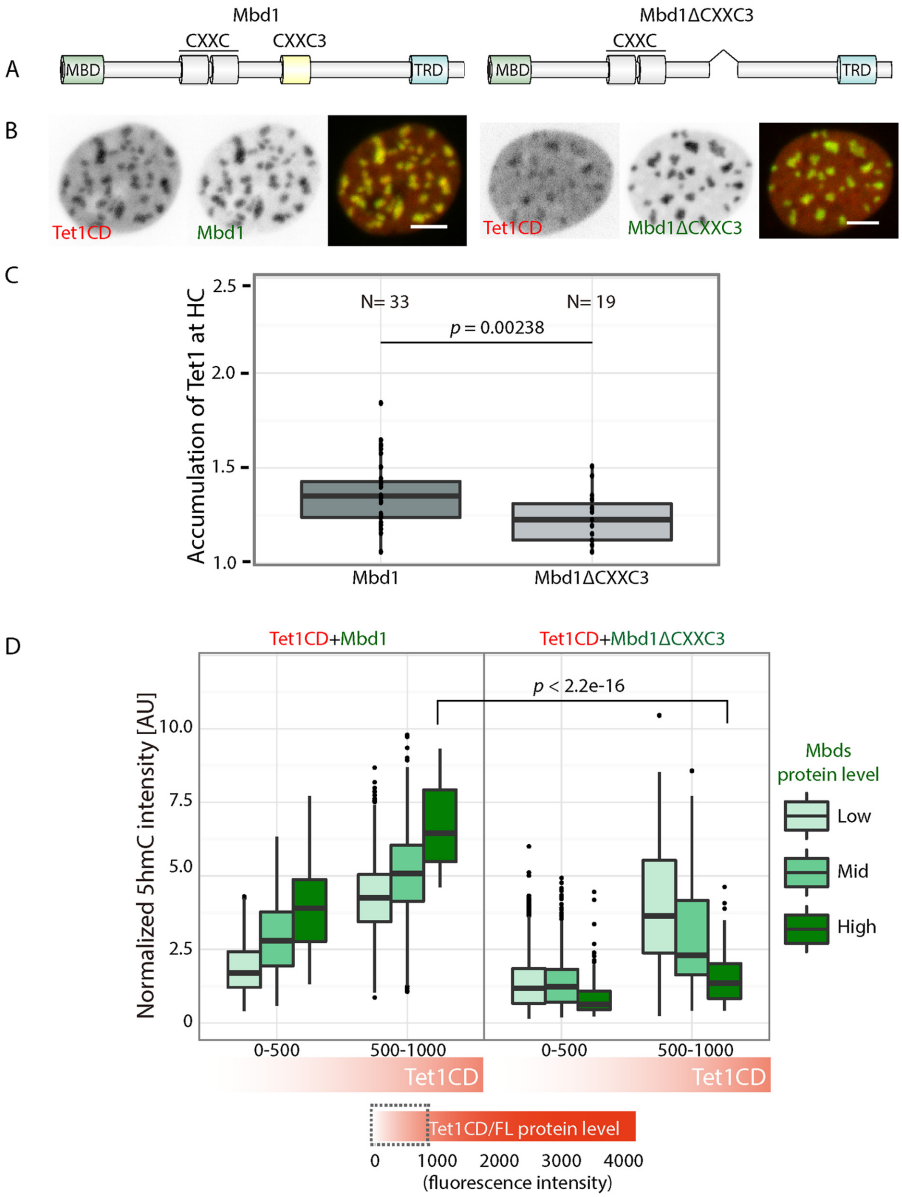

Figure 5. The CXXC3 domain of Mbd1 is necessary for Mbd1 enhanced 5hmC formation. (**A**) Structure of full length Mbd1 and Mbd1ΔCXXC3. (**B**) Examples of Tet1CD localization in the presence of Mbd1 and Mbd1ΔCXX3. MEF cells were transfected with mCherry-Tet1CD and Mbd1-GFP or GFP-Mbd1ΔCXXC3. Eight hours after transfection, the cells were imaged using confocal microscopy. Scale bars: 5 μm. (**C**) The effect of the CXXC3 on Tet1 accumulation to heterochromatic DNA. The ratio of mean intensity inside and outside heterochromatic DNA was plotted. Cell number and *P*-value of student's *t*-test are indicated on the plot. (**D**) Effect of the CXXC3 on Tet1-mediated 5hmC formation. MEF cells were transfected with mCherry-Tet1CD and Mbd1-GFP or Flag-Mbd1ΔCXXC3. Twenty-four hours after transfection, cells were stained for 5hmC. Then, cells with low Tet1CD level were used for plotting. The cells were first subgrouped by Tet1 level and then, in each group, cells were further binned by Mbd1/Mbd1ΔCXXC3 protein level. Single cell 5hmC intensity was plotted. The 5hmC intensity in the cells with high levels of Mbds and high levels of Tet1CD were used to perform student's *t*-test and *P*-values are indicated. Experiments were repeated at least three times. Cell numbers for Tet1CD + Mbd1 and Tet1CD + Mbd1ΔCXXC3 are 16757 and 2589, respectively.

accumulation of Tet1 to heterochromatic DNA. In agreement with the data from the deletion of CXXC3 domain, we found lower Tet1CD recruitment to heterochromatic DNA in the presence of Mbd1(C289,292A) (Supplementary Figure S15D). Finally, *in situ* staining showed that, comparing with Mbd1, the 5hmC levels were significantly lower in the presence of Mbd1(C289,292A) (Supplementary Figure S15E) further validating the results from the CXXC3 deletion.

Taking together, the results of both, the CXXC3 point and deletion mutants, confirmed that the binding ability of Mbd1 to unmethylated CpGs is necessary to enhance Tet1-mediated 5hmC formation.

Mbd1 isoform-dependent regulation of Tet-mediated 5hmC formation in mouse ESCs

Previous studies showed that 5hmC is highly enriched in mouse J1 ESCs due to Tet1 and Tet2 (57). In addition, Mbd1 is also present in mouse ESCs (58). To further test the effect of Mbd1 on Tet1-mediated 5hmC formation, we performed Mbd1 RNAi knockdown experiments and determined the endogenous 5hmC levels.

By western blotting, we observed that in mouse ESCs the short isoform of Mbd1 (without the CXXC3 domain) is more abundant than the long isoform (including the CXXC3 domain) (Figure 6A). After knocking down both isoforms of Mbd1 in mESCs, we observed an increase in 5hmC (Figure 6B and C; Supplementary Figure S16A and B), suggesting that, in mouse ESCs, the more abundant Mbd1ΔCXXC3 isoform, negatively regulates Tet1-mediated 5hmC formation. These results agree with the data from ectopic expression of Mbd1 and Tet1 in mouse fibroblasts, whereby we found that the Mbd1ΔCXXC3 isoform negatively impacts on Tet1-mediated 5hmC formation (Figure 5).

Subsequently, we performed isoform-specific rescue assays by ectopically expressing either of the isoforms of Mbd1 (full length and ΔCXXC3) in the Mbd1 knockdown mouse ESCs. We observed increased 5hmC levels when the cells were rescued with full length Mbd1 and a minor decrease of 5hmC with Mbd1ΔCXXC3 isoform (Figure 6D).

These results indicate that in mouse ESCs, Mbd1 regulates endogenous Tet1-mediated 5hmC formation in an isoform-dependent manner and agree with our prior isoform-specific ectopic expression data.

Tet1 and its oxidation products displace Mbd1 from heterochromatic DNA

As Mbd1 recruitment of Tet1 to heterochromatin affected Tet1 mobility (Figure 2), we analyzed next whether the converse was also true, i.e. whether Tet1 affects the mobility of Mbd1. To this end, we performed FRAP analysis. First, we tested the mobility of Mbd1 and Mbd1ΔCXXC3 in the absence of Tet1. Compared to Mbd1, Mbd1ΔCXXC3 showed faster recovery kinetics (Figure 7A), indicating that the CXXC3 domain provides an additional binding mode of Mbd1 to heterochromatic DNA.

Then, a selected heterochromatic region in cells co-expressing mCherry-tagged Tet1CD and GFP-tagged Mbd1 or Mbd1-ΔCXXC3 was photobleached using a 488 nm laser, which was shown to simultaneously bleach mCherry-tagged proteins (59). In the presence of Tet1CD, the recovery kinetics of Mbd1 was faster (Figure 7A and B, right), indicating that binding of Mbd1 to heterochromatic DNA is partially lost. In contrast, the binding kinetics of Mbd1ΔCXXC3 were not affect by Tet1 proteins (Figure 7A and B, left). As previously mentioned, Mbd1 can either bind to methylated CpG sites via its MBD domain or to unmethylated CpG sites via its CXXC3 domain, or both. Since we observed increased 5hmC levels, the MBD domain of Mbd1 might be displaced. The CXXC3 targeting sites could provide DNA docking sites for Mbd1 in the presence of Tet1 proteins with the interaction between the MBD domain of Mbd1 (as well as other Mbd1 domains) and Tet1, recruiting Tet1 to heterochromatic DNA for 5mC oxidation (Figure 7C).

Interestingly, similar binding kinetics of Tet1CD were observed with Mbd1 and Mbd1ΔCXXC3 (Figure 7B), indicating that once Tet1 binds to DNA, the interaction of Tet proteins and DNA is unaffected by Mbd1. Unlike Mbd1, which has at least two DNA binding domains, Tet1CD might only have one DNA binding site, resulting in a more simplistic protein–DNA interaction mode.

As previously mentioned, the accumulation of Tet1 to heterochromatic DNA is independent of its catalytic activity (Figure 2). To test whether the catalytic mutant of Tet1 would affect Mbd1 DNA binding, we measured the mobility of Mbd1 in the presence of Tet1CDmut and Tet1CD. While Tet1CD and Tet1CDmut had similar binding kinetics at heterochromatic DNA (Supplementary Figure S17, right), we observed an increased mobility of Mbd1 to heterochromatic DNA in the presence of Tet1CD and Tet1CDmut (Supplementary Figure S17, left), with the highest mobility in the presence of the catalytically active Tet1 variant. These results indicate that the catalytic activity of the Tet1 protein is not necessary but promotes displacement of Mbd1 from heterochromatic DNA (Supplementary Figure S17).

Previous studies have shown that Mbd1 cannot bind to 5hmC (60) and here we show that Tet1 increases the mobility of Mbd1. The initial displacement of Mbd1 from heterochromatic DNA by Tet1 might be independent of the catalytic activity of Tet proteins. However, the catalytic activity of Tet1, which leads to depletion of the Mbd1 binding substrate 5mC, enhances the fraction of mobile Mbd1 proteins to a larger extent than the catalytic inactive Tet1 variant. To further test the effect of Tet1 and its oxidation products on Mbd1 localization, high content image analysis was performed. Since we showed that the oxidation of Tet1 is dose and time dependent, we first tested the effect of different Tet1 protein levels on the localization of Mbd1 proteins. We analyzed the distribution of Mbd1 in cells with low and high Tet1 expression levels using images from *in situ* 5hmC staining (Figure 5). The homogeneous (Mbd1 freely distributed in the cell nucleus) or heterogeneous (Mbd1 accumulated at heterochromatic DNA) distributions of Mbd1 were determined by the coefficient of variation (CV) of the Mbd1 signal, which is similar as the signal standard deviation measurement (43). As mentioned earlier (Figure 2), Mbd1 accumulates at methylated heterochromatic DNA. Decreased accumulation of Mbd1 to heterochromatic DNA results in a decreased CV. The results showed that high Tet1 expression leads to increased 5hmC formation and a decreased Mbd1 CV (Supplementary Figure S18A), indicating that Mbd1 loses DNA binding sites due to 5hmC formation. However, high levels of catalytically inactive Tet1 can also decrease the localization of Mbd1 to heterochromatic DNA but with less efficiency (*P*-values 2.57×10^{-110} versus 3.67×10^{-37}) (Supplementary Figure S18A). These results indicate that high levels of Tet1 protein itself can decrease the DNA binding ability of Mbd1 to heterochromatic DNA and this is enhanced by the Tet1 oxidation products.

To test the effect of oxidation timing on localization of Mbd1 proteins, live cell microscopy of cells expressing Mbd1-GFP and mCherry-Tet1CD/CDmut or only

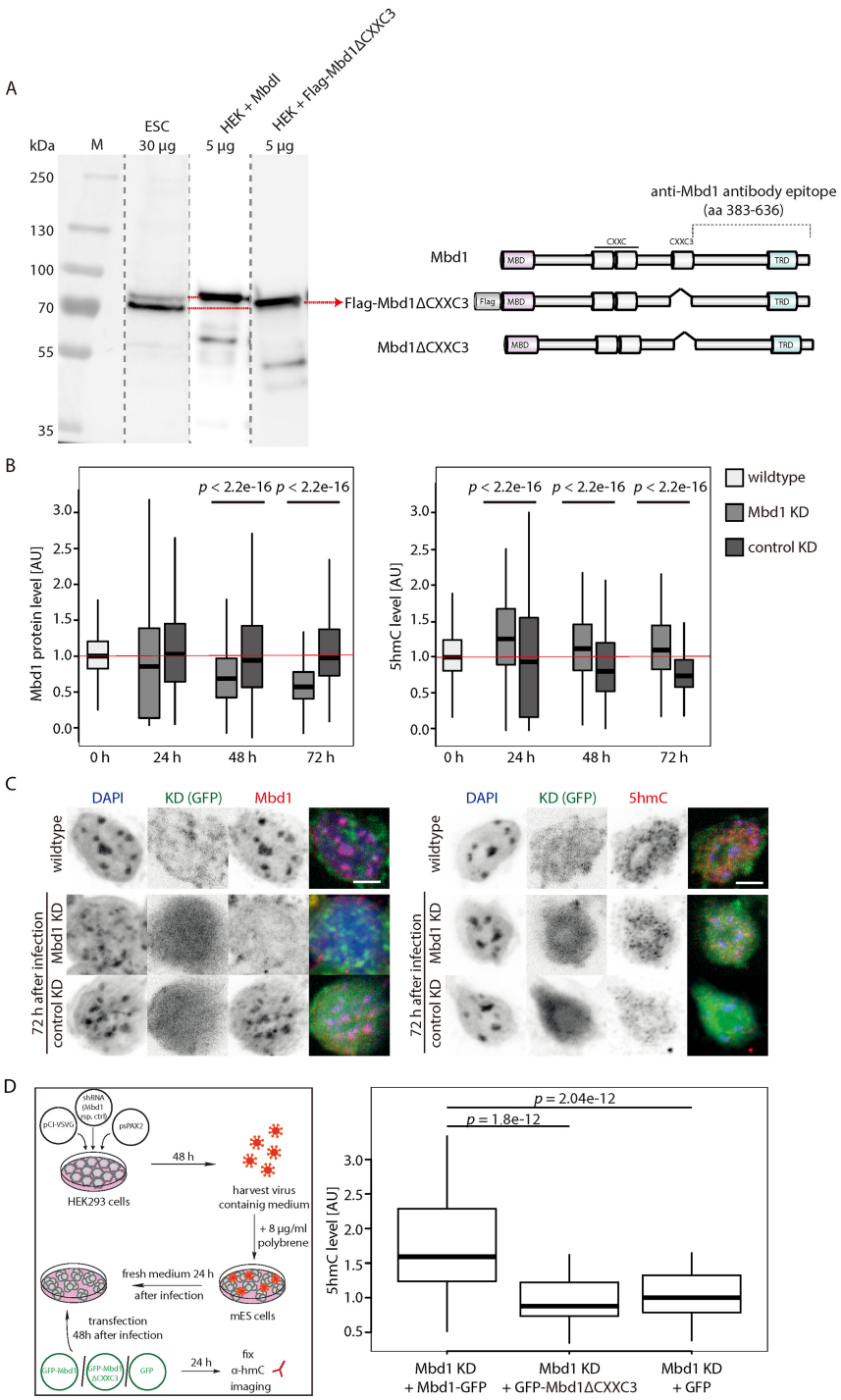

Figure 6. Mbd1 regulates 5hmC formation in mouse ESCs. (**A**) Endogenous Mbd1 isoforms in mouse ESCs compared to Mbd1 isoforms ectopically expressed in HEK cells and analyzed by western blotting with anti-Mbd1 rabbit polyclonal antibody. The first (upper) Mbd1 band in mouse ES cells corresponds to the long isoform of Mbd1, as it shows the same mobility as the ectopically expressed untagged Mbd1 (upper red line). The second (lower) Mbd1 band in ESCs corresponds to the CXXC3 deletion isoform as it migrates similarly to the ectopically expressed Mbd1ΔCXXC3. The minor difference in migration is due to the addition of the Flag tag (∼1.1 kDa, lower red line/arrow) in this construct. M: protein size marker. Exposure times are different between the lanes to compensate for the different protein levels. (**B**) Effect of Mbd1 knockdown on 5hmC formation in J1 ESCs. About 24, 48 and 72 h after lentivirus infection, the mouse ESCs were fixed and stained with Mbd1 (left) or 5hmC (right) antibodies. Then, the fluorescence signals were detected using high content screening microscopy and fluorescence intensities were further calculated using the Harmony software. The red line indicates the median fluorescence intensity of either Mbd1 or 5hmC for wild-type mouse ESCs. For each time point, at least 900 cells were used for analysis and *P*-values from *t*-tests are indicated on the plot. (**C**) Exemplary images for Mbd1 and 5hmC staining 72 h (24 and 48 h are shown in Supplementary Figure S16) after Mbd1 knockdown. Scale bars: 5 µm. (**D**) Effect of Mbd1 isoform specific rescue on 5hmC formation in mouse ESCs. A scheme of the rescue assay is shown on the left, 5hmC quantification results are shown on the right hand side. For each time point, 70 cells were used for analysis and *P*-values from *t*-tests are indicated on the plot.

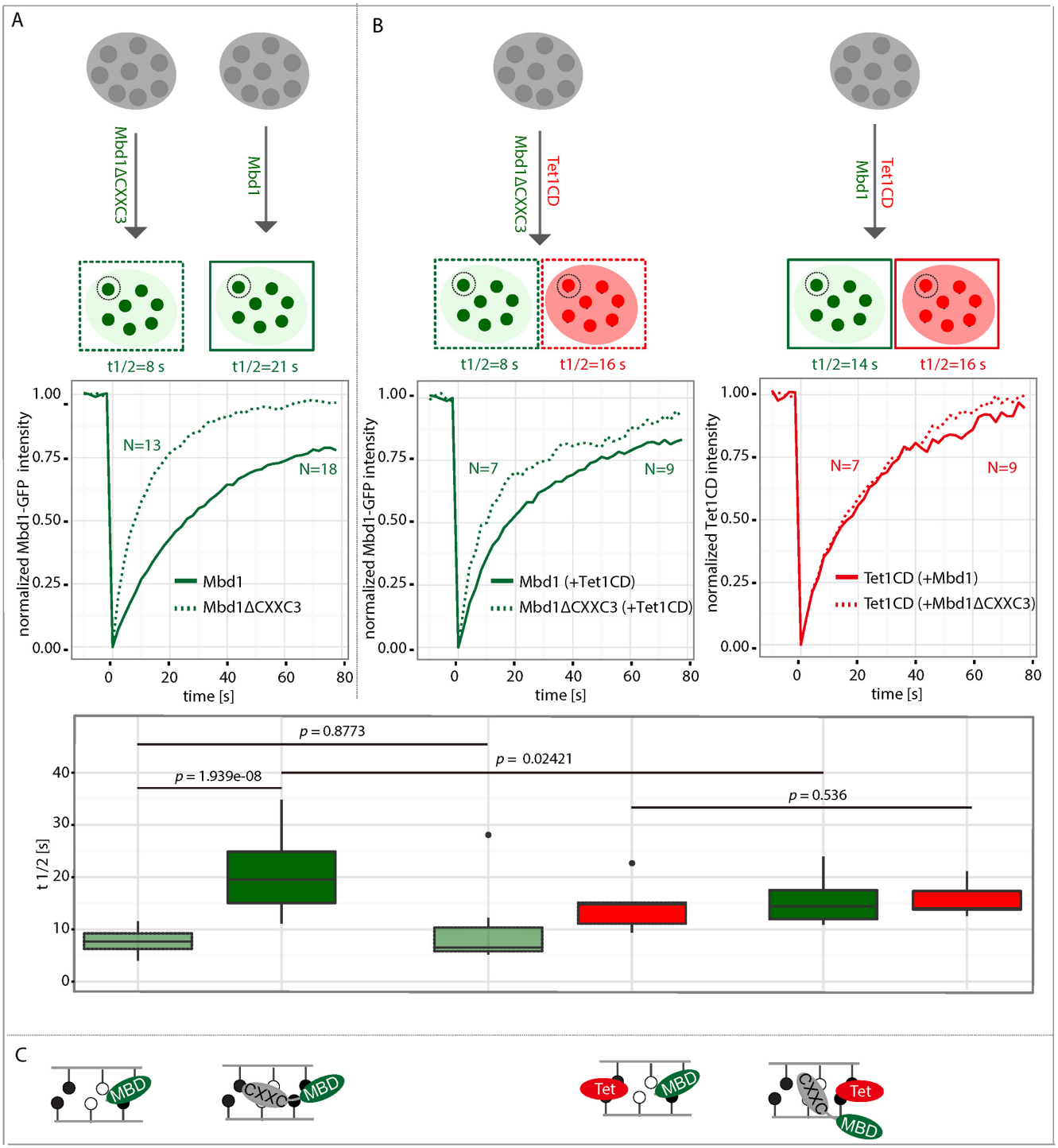

Figure 7. Tet1 displaces Mbd1 binding to heterochromatic DNA. (**A**) Mobility of Mbd1 and Mbd1ΔCXXC3. MEF cells were transfected with Mbd1-GFP or GFP-Mbd1ΔCXXC3. Eight hours after transfection, the mobility of Mbd proteins was measured by FRAP. The mean values are plotted as a recovery curve and the cell number is indicated on the plot. T-half values were extracted from mean exponential fitting. Solid and dashed lines indicate recovery curve of Mbd1ΔCXXC3 and Mbd1, respectively. (**B**) Mobility of Mbd1 (right) and Mbd1ΔCXXC3 (left) in the presence of Tet1CD. MEF cells co-expressing mCherry-Tet1CD and GFP-Mbd1 or GFP-Mbd1ΔCXX3 were used for FRAP analysis. One heterochromatic region was photobleached with a 488 nm laser, and after photobleaching the intensities of GFP and mCherry were measured. The mean values are plotted as a recovery curve and cell numbers are indicated on the plot. T-half values were extracted from the mean exponential fitting. T-half values for single cells are shown as box plots and *P*-values (Wilcoxon test) are indicated. At least two independent experiments were performed. (**C**) Scheme summarizing the Mbd1 and Tet1 binding modes to heterochromatic DNA. Black and white circles indicate methylated and unmethylated CpG, respectively.

mCherry were used for spot analysis. Eight hours after transfection, GFP and mCherry signals were detected using high content screening microscopy and spot analysis was performed as described before. To exclude Tet1 dose effects, only cells with low Tet1CD expression were used to quantify the accumulation of Mbd1 at heterochromatic DNA. As shown in Supplementary Figure S18B, the accumulation of Mbd1 at heterochromatic DNA anti-correlated with Tet1CD expression and the effect was enhanced over the oxidation time. The catalytically inactive mCherry-Tet1CD or mCherry, in contrast, did not affect the accumulation of Mbd1 at heterochromatic DNA, indicating that, at low levels of Tet1CD/CDmut, Mbd1 looses DNA binding sites due to Tet1-dependent 5hmC formation, which correlates with its oxidation time. This result is in agreement with live cell experiments using confocal microscopy (Supplementary Video 2).

Altogether, these results show that Mbd1 can be displaced from heterochromatic DNA by high levels of Tet1 protein and its oxidation product further enhances the Mbd1 displacement. However, at low levels of Tet1 protein, its oxidation product eventually causes the displacement Mbd1 from heterochromatic DNA.

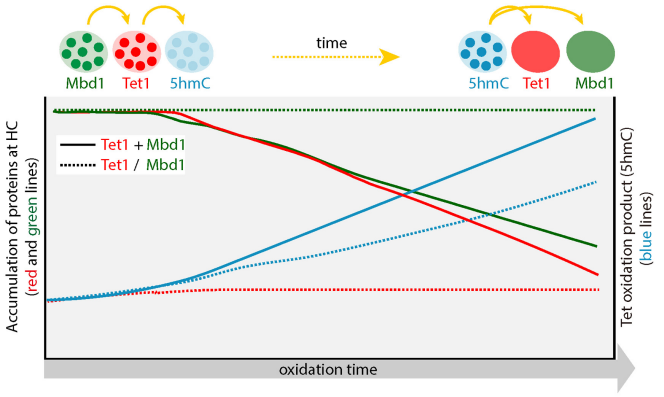

Figure 8. Summary of Tet1 and Mbd1 localization and 5hmC formation. Summary of Tet1 (red) and Mbd1 (green) localization and 5-hydroxymethylcytosine (5hmC, blue) formation. At an early time point, Mbd1 localized at heterochromatin recruits Tet1 to heterochromatic DNA and this further enhances 5hmC formation. However, once 5-methylcytosines (5mC) are modified by Tet1, both, Mbd1 and Tet1 progressively lose binding ability to heterochromatic DNA. Solid lines represent levels in cells with both Mbd1 and Tet1. Dashed lines represent levels in cells with either Mbd1 or Tet1 alone.

DISCUSSION

The dynamics of cytosine modification create a more diverse genome and regulate cellular differentiation by controlling gene expression. For proper development, the maintenance and removal of cytosine modifications have to be thoroughly regulated. Methylation of cytosines is catalyzed by Dnmts and regulation of this process has been studied extensively (61). In contrast, the regulation of methylcytosine modifiers, Tet proteins, is still highly debated and poorly understood. 5mC can be specifically recognized by methylcytosine readers and recognition of 5mC further regulates gene expression and chromatin structure (7). Methylcytosine readers Mbd2 and Mecp2 block Tet1-mediated 5mC to 5hmC conversion and further repress transcriptional noise (35). Here, we show that the MBD protein family member Mbd1, in contrast, regulates Tet1-mediated 5mC to 5hmC conversion in an isoform-dependent manner. Isoforms containing the CXXC3 domain enhance Tet1-mediated 5mC to 5hmC conversion while the ones lacking the CXXC3 domain block this process. The CXXC3 domain of Mbd1 could provide a docking site for Mbd1, which further recruits Tet1 to methylated DNA for 5mC oxidation. In summary, in stark contrast with other 5mC readers, we show here that Mbd1 enhances Tet1 activity by targeting it to heterochromatin, which contains methylated DNA. As this effect is dependent on the Mbd1-specific binding to unmethylated CpGs, we propose that this allows targeting Tet1 to CpG dense regions while not simultaneously blocking methylated CpGs from Tet1 catalytic activity.

Our study provides new insights on how methylcytosines, their readers and modifiers regulate each other. Tet1-mediated 5hmC formation is a dose and oxidation time-dependent process (Figure 8). The formation of 5hmC can be enhanced by either facilitating Tet1 binding to DNA, or by prolonging the oxidation reaction time (Figure 8). We show here that the accumulation of Mbd1 to heterochromatic DNA and its unmethylated CpG binding ability allow Mbd1 to recruit Tet1 proteins, which bind to methylated CpGs and further oxidize 5mC to 5hmC (Figure 8). However, during the oxidation process, more and more 5mC is converted to 5hmC or even further to 5fC and 5caC and it is conceivable that a progressive reduction of Tet1 protein binding to heterochromatic DNA occurs due to the absence of their substrates (Figure 8). In parallel Mbd1 proteins are displaced from heterochromatic DNA, which might be explained by the fact that 5hmC is not the preferred binding substrate for Mbd1 (Figure 8 and Supplementary Video 2).

Mbd1 has already been showed to be involved in several biological processes, such as maintaining of inactive X-chromosome (62,63) and repression of HOXA gene clustery (64), which are all correlated with DNA methylation. It would be very interesting to assess whether these processes are Mbd1 isoform dependent and whether Mbd1 regulates these processes by affecting Tet1-mediated 5mC oxidation.

Mice lacking Mbd1 develop normally and appear healthy throughout life, but are impaired in spatial learning, have decreased neurogenesis and reduced long-term potentiation in the dentate gyrus of the hippocampus (65). Similar to Mbd1 knockout mice, Tet1 knockout mice develop normally but exhibit abnormal hippocampal long-term depression and impaired memory extinction due to hypermethylation of genes targeted by Tet1 (66,67). The coinciding phenotypes of Tet1 and Mbd1 knockout mice suggest that both might be involved in neural cell function and share genomic targets. Here, we show that Mbd1 enhances Tet1-mediated 5mC to 5hmC formation, thus we suggest that Mbd1 might affect neural cell function by affecting the removal of DNA methylation marks.

Although MBD1 contains a conserved MBD domain, it was shown to have different sequence binding preferences (56,68) and also different target genes in prostate cancer cells (69) compared to MECP2. Overexpression of *MBD1* in several cancer cells lines and tissues was observed (49,70).

Since aberrant DNA methylation is a hallmark of cancer, MBD1 isoform-dependent regulation of Tet-mediated 5mC to 5hmC conversion might further contribute to the regulation of cancer-related gene expression.

SUPPLEMENTARY DATA

Supplementary Data are available at NAR Online.

ACKNOWLEDGEMENTS

We thank Katrin Schneider and Annina Scholl for generation and characterization of the RFP-PCNA expressing C2C12 stable cell line, Thomas Jenuwein for the MEF W8 cells, Howard Cedar for the *p53/Dnmt1* double knockout MEF cells, Adrian Bird for the MTF cells and plasmids, Heinrich Leonhardt for anti-Tet and GFP monoclonal antibodies as well as cell lines and Simon Linder for helping in the *in vitro* protein–protein interaction assay. We are indebted to Ingrid Grunewald, Maria Hofstätter, Manuela Milden and Anne Lehmkuhl for excellent technical assistance. We thank Francesco Natale, Kathrin Heinz, Patrick Weber and Anne Ludwig for comments on the manuscript and also Anne Ludwig for experimental advice and many helpful discussions.
Author contributions: P.Z., C.R., F.D.H., B.B., A.F. and S.J.P. performed experiments. P.Z., C.R. and F.D.H. analyzed the data. U.A.N., Y.G. and X.Z. provided materials and expertise. P.Z., C.R. and M.C.C. conceived the project and wrote the manuscript.

FUNDING

China Scholarship Council Fellowship (to P.Z.); DAAD (Deutscher Akademischer Austauschdienst) (to S.J.P.); Deutsche Forschungsgemeinschaft [DFG CA 198/7, DFG CA 198/10 to M.C.C., in part]; National Institutes of Health [RO1MH078972, R21NS095632 to X.Z., in part]. Funding for open access charge: Deutsche Forschungsgemeinschaft GRK 1657/TP1C.
Conflict of interest statement. None declared.

REFERENCES

1. Bestor,T., Laudano,A., Mattaliano,R. and Ingram,V. (1988) Cloning and sequencing of a cDNA encoding DNA methyltransferase of mouse cells. *J. Mol. Biol.*, **203**, 971–983.
2. Li,E., Bestor,T.H. and Jaenisch,R. (1992) Targeted mutation of the DNA methyltransferase gene results in embryonic lethality. *Cell*, **69**, 915–926.
3. Bird,A.P. (1980) DNA methylation and the frequency of CpG in animal DNA. *Nucleic Acids Res.*, **8**, 1499–1504.
4. Hsu,T.C., Cooper,J.E., Mace,M.L. Jr and Brinkley,B.R. (1971) Arrangement of centromeres in mouse cells. *Chromosoma*, **34**, 73–87.
5. Ludwig,A.K., Zhang,P. and Cardoso,M.C. (2016) Modifiers and readers of DNA modifications and their impact on genome structure, expression and stability in disease. *Front. Genet.*, **7**, 115.
6. Brero,A., Leonhardt,H. and Cardoso,M.C. (2006) Replication and translation of epigenetic information. *Curr. Top. Microbiol. Immunol.*, **301**, 21–44.
7. Clouaire,T. and Stancheva,I. (2008) Methyl-CpG binding proteins: specialized transcriptional repressors or structural components of chromatin? *Cell Mol. Life Sci.*, **65**, 1509–1522.
8. Voo,K.S., Carlone,D.L., Jacobsen,B.M., Flodin,A. and Skalnik,D.G. (2000) Cloning of a mammalian transcriptional activator that binds unmethylated CpG motifs and shares a CXXC domain with DNA methyltransferase, human trithorax, and methyl-CpG binding domain protein 1. *Mol. Cell. Biol.*, **20**, 2108–2121.
9. Long,H.K., Blackledge,N.P. and Klose,R.J. (2013) ZF-CxxC domain-containing proteins, CpG islands and the chromatin connection. *Biochem. Soc. Trans.*, **41**, 727–740.
10. Fujita,N., Takebayashi,S., Okumura,K., Kudo,S., Chiba,T., Saya,H. and Nakao,M. (1999) Methylation-mediated transcriptional silencing in euchromatin by methyl-CpG binding protein MBD1 isoforms. *Mol. Cell. Biol.*, **19**, 6415–6426.
11. Fujita,N., Shimotake,N., Ohki,I., Chiba,T., Saya,H., Shirakawa,M. and Nakao,M. (2000) Mechanism of transcriptional regulation by methyl-CpG binding protein MBD1. *Mol. Cell. Biol.*, **20**, 5107–5118.
12. Jorgensen,H.F., Ben-Porath,I. and Bird,A.P. (2004) Mbd1 is recruited to both methylated and nonmethylated CpGs via distinct DNA binding domains. *Mol. Cell. Biol.*, **24**, 3387–3395.
13. Thomson,J.P., Skene,P.J., Selfridge,J., Clouaire,T., Guy,J., Webb,S., Kerr,A.R., Deaton,A., Andrews,R., James,K.D. *et al.* (2010) CpG islands influence chromatin structure via the CpG-binding protein Cfp1. *Nature*, **464**, 1082–1086.
14. Farcas,A.M., Blackledge,N.P., Sudbery,I., Long,H.K., McGouran,J.F., Rose,N.R., Lee,S., Sims,D., Cerase,A., Sheahan,T.W. *et al.* (2012) KDM2B links the Polycomb Repressive Complex 1 (PRC1) to recognition of CpG islands. *Elife*, **1**, e00205.
15. Tahiliani,M., Koh,K.P., Shen,Y., Pastor,W.A., Bandukwala,H., Brudno,Y., Agarwal,S., Iyer,L.M., Liu,D.R., Aravind,L. *et al.* (2009) Conversion of 5-methylcytosine to 5-hydroxymethylcytosine in mammalian DNA by MLL partner TET1. *Science*, **324**, 930–935.
16. Maiti,A. and Drohat,A.C. (2011) Thymine DNA glycosylase can rapidly excise 5-formylcytosine and 5-carboxylcytosine: potential implications for active demethylation of CpG sites. *J. Biol. Chem.*, **286**, 35334–35338.
17. Bachman,M., Uribe-Lewis,S., Yang,X., Williams,M., Murrell,A. and Balasubramanian,S. (2014) 5-Hydroxymethylcytosine is a predominantly stable DNA modification. *Nat. Chem.*, **6**, 1049–1055.
18. Wu,H., D'Alessio,A.C., Ito,S., Xia,K., Wang,Z., Cui,K., Zhao,K., Sun,Y.E. and Zhang,Y. (2011) Dual functions of Tet1 in transcriptional regulation in mouse embryonic stem cells. *Nature*, **473**, 389–393.
19. Gao,Y., Chen,J., Li,K., Wu,T., Huang,B., Liu,W., Kou,X., Zhang,Y., Huang,H., Jiang,Y. *et al.* (2013) Replacement of Oct4 by Tet1 during iPSC induction reveals an important role of DNA methylation and hydroxymethylation in reprogramming. *Cell Stem Cell*, **12**, 453–469.
20. Ficz,G., Branco,M.R., Seisenberger,S., Santos,F., Krueger,F., Hore,T.A., Marques,C.J., Andrews,S. and Reik,W. (2011) Dynamic regulation of 5-hydroxymethylcytosine in mouse ES cells and during differentiation. *Nature*, **473**, 398–402.
21. Nestor,C.E., Ottaviano,R., Reddington,J., Sproul,D., Reinhardt,D., Dunican,D., Katz,E., Dixon,J.M., Harrison,D.J. and Meehan,R.R. (2012) Tissue type is a major modifier of the 5-hydroxymethylcytosine content of human genes. *Genome Res.*, **22**, 467–477.
22. Xu,Y., Wu,F., Tan,L., Kong,L., Xiong,L., Deng,J., Barbera,A.J., Zheng,L., Zhang,H., Huang,S. *et al.* (2011) Genome-wide regulation of 5hmC, 5mC, and gene expression by Tet1 hydroxylase in mouse embryonic stem cells. *Mol. Cell*, **42**, 451–464.
23. Jin,C., Lu,Y., Jelinek,J., Liang,S., Estecio,M.R.H., Barton,M.C. and Issa,J.P.J. (2014) TET1 is a maintenance DNA demethylase that prevents methylation spreading in differentiated cells. *Nucleic Acids Res.*, **42**, 6956–6971.
24. Bauer,C., Göbel,K., Nagaraj,N., Colantuoni,C., Wang,M., Müller,U., Kremmer,E., Rottach,A. and Leonhardt,H. (2015) Phosphorylation of TET proteins is regulated via O-GlcNAcylation by the O-Linked N-Acetylglucosamine transferase (OGT). *J. Biol. Chem.*, **290**, 4801–4812.
25. Vella,P., Scelfo,A., Jammula,S., Chiacchiera,F., Williams,K., Cuomo,A., Roberto,A., Christensen,J., Bonaldi,T., Helin,K. *et al.* (2013) Tet proteins connect the O-linked N-acetylglucosamine transferase Ogt to chromatin in embryonic stem cells. *Mol. Cell*, **49**, 645–656.
26. Konstandin,N., Bultmann,S., Szwagierczak,A., Dufour,A., Ksienzyk,B., Schneider,F., Herold,T., Mulaw,M., Kakadia,P.M., Schneider,S. *et al.* (2011) Genomic 5-hydroxymethylcytosine levels

correlate with TET2 mutations and a distinct global gene expression pattern in secondary acute myeloid leukemia. *Leukemia*, **25**, 1649–1652.
27. Blaschke,K., Ebata,K.T., Karimi,M.M., Zepeda-Martinez,J.A., Goyal,P., Mahapatra,S., Tam,A., Laird,D.J., Hirst,M., Rao,A. *et al.* (2013) Vitamin C induces Tet-dependent DNA demethylation and a blastocyst-like state in ES cells. *Nature*, **500**, 222–226.
28. Frauer,C., Rottach,A., Meilinger,D., Bultmann,S., Fellinger,K., Hasenöder,S., Wang,M., Qin,W., Söding,J., Spada,F. *et al.* (2011) Different binding properties and function of CXXC zinc finger domains in Dnmt1 and Tet1. *PLoS One*, **6**, e16627.
29. Ko,M., An,J., Bandukwala,H.S., Chavez,L., Aijö,T., Pastor,W.a., Segal,M.F., Li,H., Koh,K.P., Lähdesmäki,H. *et al.* (2013) Modulation of TET2 expression and 5-methylcytosine oxidation by the CXXC domain protein IDAX. *Nature*, **497**, 122–126.
30. Hendrich,B. and Bird,A. (1998) Identification and characterization of a family of mammalian methyl-CpG binding proteins. *Mol. Cell. Biol.*, **18**, 6538–6547.
31. Becker,A., Allmann,L., Hofstatter,M., Casa,V., Weber,P., Lehmkuhl,A., Herce,H.D. and Cardoso,M.C. (2013) Direct homo- and hetero-interactions of MeCP2 and MBD2. *PLoS One*, **8**, e53730.
32. Brero,A., Easwaran,H.P., Nowak,D., Grunewald,I., Cremer,T., Leonhardt,H. and Cardoso,M.C. (2005) Methyl CpG-binding proteins induce large-scale chromatin reorganization during terminal differentiation. *J. Cell Biol.*, **169**, 733–743.
33. Jost,K.L., Rottach,A., Milden,M., Bertulat,B., Becker,A., Wolf,P., Sandoval,J., Petazzi,P., Huertas,D., Esteller,M. *et al.* (2011) Generation and characterization of rat and mouse monoclonal antibodies specific for MeCP2 and their use in X-inactivation studies. *PLoS One*, **6**, e26499.
34. Casas-Delucchi,C.S., Becker,A., Bolius,J.J. and Cardoso,M.C. (2012) Targeted manipulation of heterochromatin rescues MeCP2 Rett mutants and re-establishes higher order chromatin organization. *Nucleic Acids Res.*, **40**, e176.
35. Ludwig,A.K., Zhang,P., Hastert,F.D., Meyer,S., Rausch,C., Herce,H.D., Muller,U., Lehmkuhl,A., Hellmann,I., Trummer,C. *et al.* (2017) Binding of MBD proteins to DNA blocks Tet1 function thereby modulating transcriptional noise. *Nucleic Acids Res.*, **45**, 2438–2457.
36. Leonhardt,H., Rahn,H.P., Weinzierl,P., Sporbert,A., Cremer,T., Zink,D. and Cardoso,M.C. (2000) Dynamics of DNA replication factories in living cells. *J. Cell Biol.*, **149**, 271–280.
37. Qin,W., Leonhardt,H. and Spada,F. (2011) Usp7 and Uhrf1 control ubiquitination and stability of the maintenance DNA methyltransferase Dnmt1. *J. Cell. Biochem.*, **112**, 439–444.
38. Smrt,R.D., Szulwach,K.E., Pfeiffer,R.L., Li,X.K., Guo,W.X., Pathania,M., Teng,Z.Q., Luo,Y.P., Peng,J.M., Bordey,A. *et al.* (2010) MicroRNA miR-137 regulates neuronal maturation by targeting ubiquitin ligase mind bomb-1. *Stem Cells*, **28**, 1060–1070.
39. Agarwal,N., Hardt,T., Brero,A., Nowak,D., Rothbauer,U., Becker,A., Leonhardt,H. and Cardoso,M.C. (2007) MeCP2 interacts with HP1 and modulates its heterochromatin association during myogenic differentiation. *Nucleic Acids Res.*, **35**, 5402–5408.
40. Guy,J., Hendrich,B., Holmes,M., Martin,J.E. and Bird,A. (2001) A mouse Mecp2-null mutation causes neurological symptoms that mimic Rett syndrome. *Nat. Genet.*, **27**, 322–326.
41. Peters,A.H., O'Carroll,D., Scherthan,H., Mechtler,K., Sauer,S., Schofer,C., Weipoltshammer,K., Pagani,M., Lachner,M., Kohlmaier,A. *et al.* (2001) Loss of the Suv39h histone methyltransferases impairs mammalian heterochromatin and genome stability. *Cell*, **107**, 323–337.
42. Lande-Diner,L., Zhang,J., Ben-Porath,I., Amariglio,N., Keshet,I., Hecht,M., Azuara,V., Fisher,A.G., Rechavi,G. and Cedar,H. (2007) Role of DNA methylation in stable gene repression. *J. Biol. Chem.*, **282**, 12194–12200.
43. Casas-Delucchi,C.S., van Bemmel,J.G., Haase,S., Herce,H.D., Nowak,D., Meilinger,D., Stear,J.H., Leonhardt,H. and Cardoso,M.C. (2012) Histone hypoacetylation is required to maintain late replication timing of constitutive heterochromatin. *Nucleic Acids Res.*, **40**, 159–169.
44. Becker,A., Zhang,P., Allmann,L., Meilinger,D., Bertulat,B., Eck,D., Hofstaetter,M., Bartolomei,G., Hottiger,M.O., Schreiber,V. *et al.* (2016) Poly(ADP-ribosyl)ation of methyl CpG binding domain protein 2 regulates chromatin structure. *J. Biol. Chem.*, **291**, 4873–4881.
45. Hooper,M., Hardy,K., Handyside,A., Hunter,S. and Monk,M. (1987) Hprt-deficient (Lesch-Nyhan) mouse embryos derived from germline colonization by cultured-cells. *Nature*, **326**, 292–295.
46. Herce,H.D., Casas-Delucchi,C.S. and Cardoso,M.C. (2013) New image colocalization coefficient for fluorescence microscopy to quantify (bio-)molecular interactions. *J. Microsc.*, **249**, 184–194.
47. Ito,S., D'Alessio,A.C., Taranova,O.V., Hong,K., Sowers,L.C. and Zhang,Y. (2010) Role of Tet proteins in 5mC to 5hmC conversion, ES-cell self-renewal and inner cell mass specification. *Nature*, **466**, 1129–1133.
48. Hashimoto,H., Pais,J.E., Zhang,X., Saleh,L., Fu,Z.Q., Dai,N., Correa,I.R. Jr., Zheng,Y. and Cheng,X. (2014) Structure of a Naegleria Tet-like dioxygenase in complex with 5-methylcytosine DNA. *Nature*, **506**, 391–395.
49. Hu,L., Li,Z., Cheng,J., Rao,Q., Gong,W., Liu,M., Shi,Y.G., Zhu,J., Wang,P. and Xu,Y. (2013) Crystal structure of TET2-DNA complex: insight into TET-mediated 5mC oxidation. *Cell*, **155**, 1545–1555.
50. Muller,U., Bauer,C., Siegl,M., Rottach,A. and Leonhardt,H. (2014) TET-mediated oxidation of methylcytosine causes TDG or NEIL glycosylase dependent gene reactivation. *Nucleic Acids Res.*, **42**, 8592–8604.
51. Hu,L., Lu,J., Cheng,J., Rao,Q., Li,Z., Hou,H., Lou,Z., Zhang,L., Li,W., Gong,W. *et al.* (2015) Structural insight into substrate preference for TET-mediated oxidation. *Nature*, **527**, 118–122.
52. Sarraf,S.A. and Stancheva,I. (2004) Methyl-CpG binding protein MBD1 couples histone H3 methylation at lysine 9 by SETDB1 to DNA replication and chromatin assembly. *Mol. Cell*, **15**, 595–605.
53. Weidtkamp-Peters,S., Rahn,H.P., Cardoso,M.C. and Hemmerich,P. (2006) Replication of centromeric heterochromatin in mouse fibroblasts takes place in early, middle, and late S phase. *Histochem. Cell Biol.*, **125**, 91–102.
54. Easwaran,H.P., Schermelleh,L., Leonhardt,H. and Cardoso,M.C. (2004) Replication-independent chromatin loading of Dnmt1 during G2 and M phases. *EMBO Rep.*, **5**, 1181–1186.
55. Lai,J.S. and Herr,W. (1992) Ethidium bromide provides a simple tool for identifying genuine DNA-independent protein associations. *Proc. Natl. Acad. Sci. U.S.A.*, **89**, 6958–6962.
56. Clouaire,T., de Las Heras,J.I., Merusi,C. and Stancheva,I. (2010) Recruitment of MBD1 to target genes requires sequence-specific interaction of the MBD domain with methylated DNA. *Nucleic Acids Res.*, **38**, 4620–4634.
57. Dawlaty,M.M., Breiling,A., Le,T., Raddatz,G., Barrasa,M.I., Cheng,A.W., Gao,Q., Powell,B.E., Li,Z., Xu,M. *et al.* (2013) Combined deficiency of Tet1 and Tet2 causes epigenetic abnormalities but is compatible with postnatal development. *Dev. Cell*, **24**, 310–323.
58. Kobayakawa,S., Miike,K., Nakao,M. and Abe,K. (2007) Dynamic changes in the epigenomic state and nuclear organization of differentiating mouse embryonic stem cells. *Genes Cells*, **12**, 447–460.
59. Sporbert,A., Domaing,P., Leonhardt,H. and Cardoso,M.C. (2005) PCNA acts as a stationary loading platform for transiently interacting Okazaki fragment maturation proteins. *Nucleic Acids Res.*, **33**, 3521–3528.
60. Hashimoto,H., Liu,Y., Upadhyay,A.K., Chang,Y., Howerton,S.B., Vertino,P.M., Zhang,X. and Cheng,X. (2012) Recognition and potential mechanisms for replication and erasure of cytosine hydroxymethylation. *Nucleic Acids Res.*, **40**, 4841–4849.
61. Denis,H., Ndlovu,M.N. and Fuks,F. (2011) Regulation of mammalian DNA methyltransferases: a route to new mechanisms. *EMBO Rep.*, **12**, 647–656.
62. Minkovsky,A., Sahakyan,A., Rankin-Gee,E., Bonora,G., Patel,S. and Plath,K. (2014) The Mbd1-Atf7ip-Setdb1 pathway contributes to the maintenance of X chromosome inactivation. *Epigenet. Chromatin*, **7**, 12.
63. Sharp,A.J., Stathaki,E., Migliavacca,E., Brahmachary,M., Montgomery,S.B., Dupre,Y. and Antonarakis,S.E. (2011) DNA methylation profiles of human active and inactive X chromosomes. *Genome Res.*, **21**, 1592–1600.
64. Sakamoto,Y., Watanabe,S., Ichimura,T., Kawasuji,M., Koseki,H., Baba,H. and Nakao,M. (2007) Overlapping roles of the methylated DNA-binding protein MBD1 and polycomb group proteins in transcriptional repression of HOXA genes and heterochromatin foci formation. *J. Biol. Chem.*, **282**, 16391–16400.

65. Zhao,X., Ueba,T., Christie,B.R., Barkho,B., McConnell,M.J., Nakashima,K., Lein,E.S., Eadie,B.D., Willhoite,A.R., Muotri,A.R. *et al.* (2003) Mice lacking methyl-CpG binding protein 1 have deficits in adult neurogenesis and hippocampal function. *Proc. Natl. Acad. Sci. U.S.A.*, **100**, 6777–6782.
66. Rudenko,A., Dawlaty,M.M., Seo,J., Cheng,A.W., Meng,J., Le,T., Faull,K.F., Jaenisch,R. and Tsai,L.H. (2013) Tet1 is critical for neuronal activity-regulated gene expression and memory extinction. *Neuron*, **79**, 1109–1122.
67. Zhang,R.R., Cui,Q.Y., Murai,K., Lim,Y.C., Smith,Z.D., Jin,S., Ye,P., Rosa,L., Lee,Y.K., Wu,H.P. *et al.* (2013) Tet1 regulates adult hippocampal neurogenesis and cognition. *Cell Stem Cell*, **13**, 237–245.
68. Baker,S.A., Chen,L., Wilkins,A.D., Yu,P., Lichtarge,O. and Zoghbi,H.Y. (2013) An AT-hook domain in MeCP2 determines the clinical course of Rett syndrome and related disorders. *Cell*, **152**, 984–996.
69. Yaqinuddin,A., Abbas,F., Naqvi,S.Z., Bashir,M.U., Qazi,R. and Qureshi,S.A. (2008) Silencing of MBD1 and MeCP2 in prostate-cancer-derived PC3 cells produces differential gene expression profiles and cellular phenotypes. *Biosci. Rep.*, **28**, 319–326.
70. Patra,S.K., Patra,A., Zhao,H., Carroll,P. and Dahiya,R. (2003) Methyl-CpG-DNA binding proteins in human prostate cancer: expression of CXXC sequence containing MBD1 and repression of MBD2 and MeCP2. *Biochem. Biophys. Res. Commun.*, **302**, 759–766.